



Università degli Studi di Napoli Federico II
SCUOLA POLITECNICA E DELLE SCIENZE DI BASE

DIPARTIMENTO DI INGEGNERIA INDUSTRIALE
Corso di Laurea in Ingegneria Aerospaziale

Tesi di Laurea Magistrale
in
Ingegneria Aerospaziale ed Astronautica

**Development of a Java Framework for
Parametric Aircraft Design**

The Performance Analysis Module

Candidato:
Vittorio Trifari
Matricola M53/411

Relatori:
Prof. Fabrizio Nicolosi
Prof. Agostino De Marco

Abstract

This thesis has the main purpose of providing a comprehensive overview about the development, in Java, of a software dedicated to the preliminary design of an aircraft, focusing on the performance analysis module.

The point of view from which this subject will be observed expects first to define methodologies and theoretical aspects necessary for the examined performance calculation for then show, in more detail, the implementation of the latter within the software; this will be seen both from the point of view of the developer, through a detailed explanation of the architecture of the different calculation modules, both of a potential user developer, by showing some commented examples of use supplied with graphical and numerical results suitable, among other things, also to the validation of calculations performed.

Sommario

Questo lavoro di tesi ha lo scopo principale di fornire una panoramica esaustiva circa lo sviluppo, in ambiente Java, di un software dedicato al progetto preliminare di un aeromobile, concentrandosi sull'aspetto dell'analisi delle performance.

Il punto di vista con il quale verrà affrontato questo argomento prevede dapprima di inquadrare le metodologie e gli aspetti teorici necessari per la stima delle performance in esame per poi mostrare, più nel dettaglio, l'implementazione di questi ultimi all'interno del software; ciò sia dal punto di vista dello sviluppatore, attraverso la spiegazione dettagliata dell'architettura dei vari moduli di calcolo, sia dal punto di vista di un potenziale utente, tramite alcuni esempi d'uso commentati e corredati di risultati grafici e numerici atti, tra l'altro, anche alla validazione dei calcoli svolti.

CONTENTS

1 Software overview	5
1.1 Main purposes	5
1.2 Input file structure	5
1.3 The Core Package	5
1.4 Aircraft model creation	5
1.5 The Graphical User Interface	5
2 Payload-Range	7
2.1 Theoretical background	7
2.2 Java class architecture	11
2.3 Case study: ATR-72 and B747-100B	14
3 Specific Range and Cruise Grid	27
3.1 Theoretical background	27
3.2 Java class architecture	32
3.3 Case study: ATR-72 and B747-100B	34
4 High lift devices effects	43
4.1 Theoretical background	44
4.1.1 ΔC_{l0} and ΔC_{L0} calculation	47
4.1.2 $\Delta C_{l\max}$ and $\Delta C_{L\max}$ calculation for flaps and slats	50
4.1.3 $C_{l\alpha,\text{flap}}$ and $C_{L\alpha,\text{flap}}$ calculation	50
4.1.4 $\Delta\alpha_{\text{stall}}$ calculation for flaps and slats	50
4.1.5 Further effects calculations	50
4.2 Java class architecture	50
4.3 Case study: ATR-72 and B747-100B	50
5 Take-off performance	51
5.1 Theoretical background	51
5.2 Java class architecture	51
5.3 Case study: B747-100B	51
Appendices	

A HDF database creation and reading	55
A.1 Creation of a database using MATLAB	55
A.2 Reading data from an HDF database in JPAD	58
Bibliography	60
Glossary	63
Acronyms	65
List of symbols	67

Chapter **1**

SOFTWARE OVERVIEW

- 1.1 Main purposes**
- 1.2 Input file structure**
- 1.3 The Core Package**
- 1.4 Aircraft model creation**
- 1.5 The Graphical User Interface**

Chapter 2

Payload-Range

The Payload-Range diagram is a very important resource in aircrafts design because it allows to illustrate an aircraft operational limits by showing the trade-off relationship between the payload that can be carried and the range that can be flown; moreover, in synergy with the D.O.C. diagram, it's very useful to the future aircraft customers to have an idea of expected profits derived by their investment.

Payload-Range is also a key feature of the design requirements so it's possible to state that its relevance is felt through all the preliminary and conceptual design phases.

2.1 Theoretical background

To better understand the theoretical background behind this diagram, the first step is to focus the attention upon the link between the range and the fuel consumption, which is influenced by aircraft weight through Breguet formulas.

It's possible to imagine, at first, an aircraft in which payload and fuel weights can be managed at will, so that, in this completely flexible aircraft, the more the required range is, the less is the payload in order to carry more fuel at a specified maximum take-off weight; this leads to the diagram in figure 3.1.

Because the payload is carried in the fuselage while the fuel is carried in wing tanks, the more the payload, the more the weight in the fuselage; this means that wings are incrementally more bending loaded so that a heavier structure is required. However, in this way the operating empty weight grows up limiting the payload the aircraft can carry, at that maximum take-off and fuel weights, for that range; the consequence of this is that, in particular for long range missions, the payload is too low, providing low profits.

In order to avoid this situation it's possible to decide, preventively, the maximum payload weight the aircraft can carry in fuselage so that the maximum bending load for wings and, in consequence their structural weight, is set; this particular weight is named maximum zero fuel weight (MZFW).

As a result of this, the previous diagram changes in the one reported in figure 3.2 which

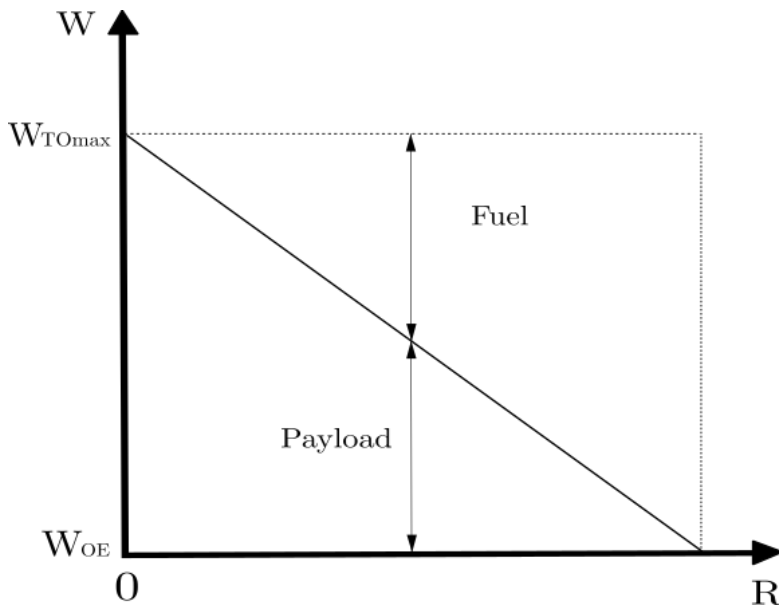


Figure 2.1 Payload-Range for a completely flexible aircraft

starts with the maximum zero fuel weight and keep it constant until the maximum take-off weight is reached. From this point on, the far the aircraft have to go, the more the fuel it needs, but, since the maximum take-off weight is set, the only way to increase fuel weight is to reduce the payload; this condition is represented by the second segment of the diagram and, along this, the aircraft weight is always equal to the maximum take-off weight. With further increase of the required range for the aircraft, the fuel tanks maximum capacity will be reached prevent to store more fuel; the only solution at this problem is to put the additional fuel into the fuselage, reducing, consequently, the payload weight in order to respect the maximum zero fuel weight limitation. Along this last segment the payload weight decreases more rapidly with increasing range reaching, ideally, the value of zero at which the flight mission is useless; moreover the aircraft weight is not equal to the maximum take-off weight anymore but to a lower one.

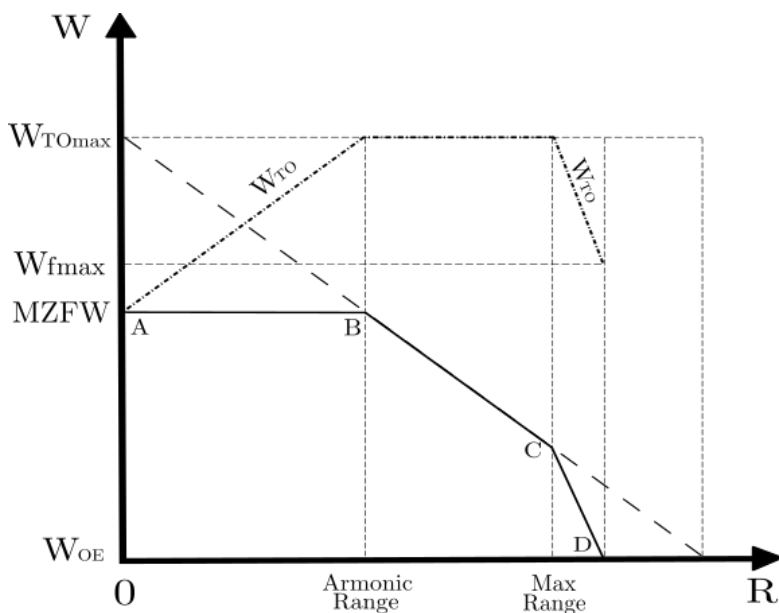


Figure 2.2 Payload-Range with MZFW limitation

Now that the theory behind the Payload-Range is explained, it's interesting to see how to build up the diagram. For this purpose at least the preliminary weight estimation has to be done in order to know the value of the following weights.

- W_{TO}
- W_{OE}
- $W_{Payload}$

Furthermore four fundamental couples of payload and range values have to be defined:

- Point A, in which the payload is the maximum allowed and the range is zero.
- Point B, in which the maximum range, with maximum take-off weight and maximum payload, is reached. This range value is called Armoinc Range.
- Point C, in which the fuel tanks full capacity is reached with a payload lower than the maximum one and still the maximum take-off weight.
- Point D, in which the take-off weight decreases because of the reduction of payload to zero in order to store more fuel in the fuselage.

Since point A is very simple to obtain, it's more interesting to analyze how to calculate points B, C and D coordinates.

For point B it's necessary to focus the attention upon Breguet formulas in order to calculate the maximum range the aircraft can fly at maximum take-off weight with maximum payload; these are different for jet or propeller aircraft and can be written as follow, with R in km, SFC in $\frac{\text{lb}}{\text{hp}\cdot\text{h}}$ and SFCJ in $\frac{\text{lb}}{\text{lb}\cdot\text{h}}$.

$$R = 603.5 \cdot \left(\frac{\eta_p}{SFC} \right)_{cruise} \cdot \left(\frac{L}{D} \right)_{cruise} \cdot \ln \left(\frac{W_i}{W_f} \right) \quad \text{if propeller engine driven} \quad (2.1a)$$

$$R = \left(\frac{V}{SFCJ} \right)_{cruise} \cdot \left(\frac{L}{D} \right)_{cruise} \cdot \ln \left(\frac{W_i}{W_f} \right) \quad \text{if jet engine driven} \quad (2.1b)$$

Knowing the specific fuel consumption, the aerodynamic and propeller efficiency, or speed for jet aircraft, in cruise condition, the only unknown left for calculate the range is the weight ratio. In order to calculate this it's necessary to start by evaluating the amount of fuel the airplane can take on board, at maximum take-off weight and maximum payload, with the following formula.

$$W_{TO,max} = W_{OE} + W_{payload,max} + W_{fuel} \quad (2.2)$$

Once the used fuel weight is known, it's possible to use the fuel fraction method from the weight estimation design phase in order to find the total weight ratio across the entire aircraft mission.

$$W_{\text{fuel}} = (1 - M_{ff}) \cdot W_{TO} \quad (2.3)$$

M_{ff} is the fuel fraction of the entire mission profile given by the following expression.

$$M_{ff} = \frac{W_1}{W_{TO}} \cdot \frac{W_2}{W_1} \cdot \frac{W_3}{W_2} \cdot \frac{W_4}{W_3} \cdot \frac{W_5}{W_4} \cdot \frac{W_6}{W_5} \cdot \frac{W_7}{W_6} \cdot \frac{W_8}{W_7} \cdot \frac{W_9}{W_8} \cdot \frac{W_{10}}{W_9} \cdot \frac{W_{\text{final}}}{W_{10}} \quad (2.4)$$

From this point on, it's necessary to have a table, like the one of table 3.1, in which all weight ratios can be found statistically except for cruise, alternate cruise and loiter phases; these three unknown ratios are those that build up the Breguet weight ratio required by the range formula.

Airplane type	Start, Warm-up	Taxi	Take-off	Brief descent	Brief climb	Landing, Taxi and Shutdown
Homebuilt	0,998	0,998	0,998	0,995	0,995	0,995
Single Engine	0,995	0,997	0,998	0,992	0,993	0,993
Twin Engine	0,992	0,996	0,996	0,990	0,992	0,992
Agricultural	0,996	0,995	0,996	0,998	0,999	0,998
Business Jets	0,990	0,995	0,995	0,980	0,990	0,992
Regional TBP's	0,990	0,995	0,995	0,985	0,985	0,995
Transport Jets	0,990	0,990	0,995	0,980	0,990	0,992
Mil. Trainers	0,990	0,990	0,990	0,980	0,990	0,995
Fighters	0,990	0,990	0,990	0,960-0,900	0,990	0,995
Mil.Patrol,Bmb and Trspt	0,990	0,990	0,995	0,980	0,990	0,992
Flying boats,Amph. and Floats	0,992	0,990	0,996	0,985	0,990	0,990
Supersonic Cruise	0,990	0,995	0,995	0,920-0,870	0,985	0,992

Table 2.1 Suggested fuel fractions

For the evaluation of point C, similar steps have to be followed with the difference that, in this case, the fuel is the maximum that the wing tanks can store and the payload is the unknown of the (2.5).

$$W_{TO,\max} = W_{OE} + W_{\text{payload}} + W_{\text{fuel,max}} \quad (2.5)$$

From this equation it's possible to calculate point C ordinate, while for the range abscissa the same procedure used for point B range has to be followed with the difference that now it's necessary to use the fuel weight relative to the maximum fuel tank capacity which is known from the wing fuel tank design.

Finally for point D, the payload is set at zero so that is possible to evaluate the WTO, relative to maximum fuel weight with no passengers, from the following equation.

$$W_{TO} = W_{OE} + W_{\text{fuel,max}} \quad (2.6)$$

This new take-off weight generates a lower M_{ff} , from fuel fraction equation, which leads to a bigger weight ratio to be used in Breguet formulas with the result of a bigger range.

2.2 Java class architecture

In this paragraph the implementation in the JPAD software of the Payload-Range diagram, through the `PayloadRangeCalc` Java class, is presented. The idea has been to create a dedicated Java class which is demanded of the calculation of the four couple of range and payload values presented before; moreover it has to confront the user chosen Mach number condition with the best range one and to parametrize the analysis at different maximum take-off weight in order to help users making design decisions about different version of the same aircraft.

The class core consists of the following three principal methods which have to evaluate points B, C and D coordinates using the procedure explained before.

- `calcRangeAtMaxPayload`
- `calcRangeAtMaxFuel`
- `calcRangeAtZeroPayload`

Each of these requires in input the table 3.2 data, a database which collects all data from table 3.1, named *FuelFractions.h5*, and an engine database, for turboprop or turbofan, in which all specific fuel consumption values, at given Mach number and altitude, are stored.

From this point on, the evaluation of (2.2), (2.5) and (2.6), for each method, and of (2.3), for all of them, is performed in order to set up the following calculations and to obtain the unknown value of the payload in point C case; after that the fuel fractions database is read in order to obtain all known data necessary to calculate the required weight ratio to be used in (??) or (??) depending on the aircraft engine type. It's important to highlight that the database

maxTakeOffMass	Maximum take-off mass
sweepHalfChordEquivalent	Equivalent wing sweep angle at half chord
surface	Wing surface
cd0	Wing c_{D0}
oswald	Wing oswald factor
cl	The current lift coefficient in cruise configuration
ar	Wing aspect ratio
tcMax	Mean maximum thickness of the wing
byPassRatio	Engine by-pass ratio (when needed)
eta	Propeller efficiency (when needed)
altitude	Cruise altitude
currentMach	The actual Mach number during cruise
isBestRange	A boolean variable that is true if the evaluation of the best range condition is performed, otherwise it's false

Table 2.2 Input data

reading process is made up so that it can recognize all different kind of aircraft from table 3.1 and read the related line values.

Since each method has to compare the chosen Mach number condition with the best range one, the boolean variable presented before is used in order to distinguish between different application cases; in this way, when the user specify the aircraft engine type and the boolean variable, the method reads the specific fuel consumption value, at given Mach number and altitude, from the related engine database and performs the calculation of the lift and drag wing coefficients which are then used to obtain the aerodynamic efficiency value. At this point is possible to calculate the range that represents point B, C or D abscissa.

It should be noted that, in case of a true value of the boolean variable, the evaluation of the lift and drag wing coefficients, as well as the best range Mach number that replaces the user chosen one, is performed by calculating the parabolic drag polar characteristic points and choosing those that maximizes the range (point E for the turboprop and point A for the turbofan); whereas for a false value of the boolean variable, the lift coefficient is calculated by using the current flight condition angle of attack into the linear part of the wing lift curve, while the drag coefficient is evaluated from the aircraft total drag polar taking also into account potential wave drag sources.

Now that all points coordinates are known, the two following methods are demanded to build up abscissas and ordinates values arrays to be used in plotting the diagram.

- `createRangeArray`
- `createPayloadArray`

Range Array	Payload Array
0,0	Maximum payload, in number of passengers
calcRangeAtMaxPayload output	Maximum payload, in number of passengers
calcRangeAtMaxFuel output	Payload calculated in calcRangeAtMaxFuel
calcRangeAtZeroPayload output	0,0

Table 2.3 Payload and range array components

They use the Java `List` interface to generate an ordered collection of values which are then populated with the following values.

Finally the two arrays are used as input, together with another one from the best range condition analysis, for the last method, named `createPayloadRangeCharts_Mach`, that has to plot the diagram; this uses the `JFreeChart` Java library to generate a `.png` output image into the output folder of the software and is also able to create a `.tikz` version of the diagram to be used in `LATEX`.

As said before, this class finds another purpose in parameterizing the diagram in different maximum take-off weight conditions. To do that, the three core methods are used again inside a new one, named `createPayloadRangeMatrices`, which implements a recursive calculation of the three points coordinates at different maximum take-off mass conditions generated by decreasing the original mass by 5% until it reaches a total decrease of 20%. This new method requires the same input data reported in table 3.2 except for the maximum take-off mass which is generated inside the method itself.

The output matrices are then used in a plotting method, equivalent to previous one but named `createPayloadRangeCharts_MaxTakeOffMass`, which generates the `.png` and `.tikz` output images by receiving as input two matrices and not two arrays as before.

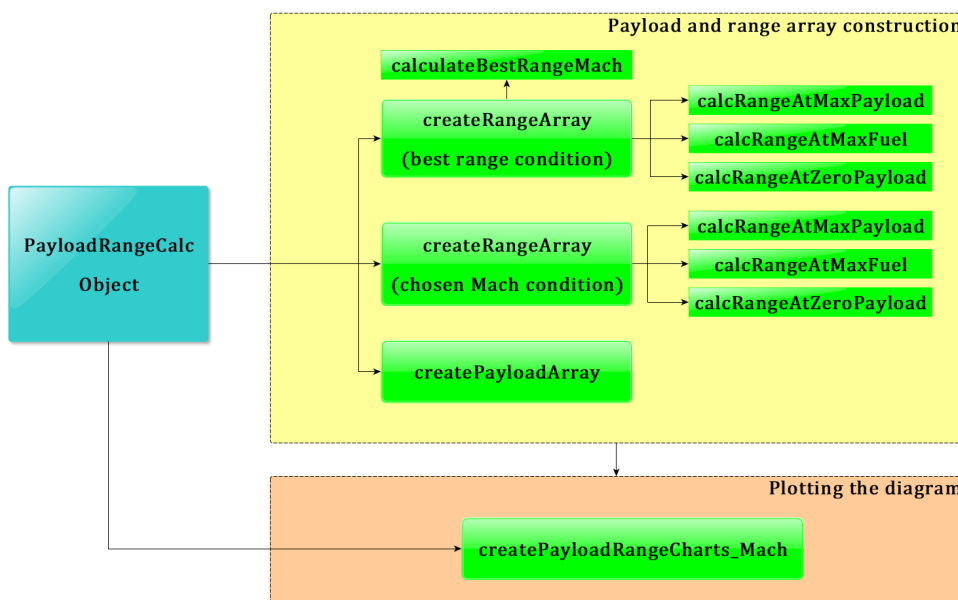


Figure 2.3 Payload-Range java class flowchart for best range and chosen Mach conditions comparison

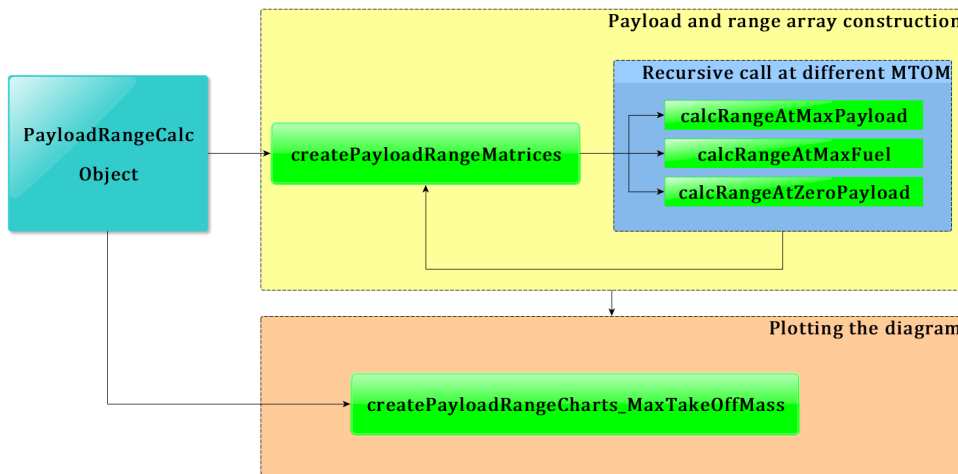


Figure 2.4 Payload-Range java class flowchart for maximum take-off mass parameterization

2.3 Case study: ATR-72 and B747-100B

With the purpose of validating calculations presented before, two case studies have been taken into account; the first one is on the ATR-72 and the second one on the B747-100B.

The ATR-72, made by the French-Italian aircraft manufacturer ATR, is a stretched variant of the original ATR-42 that entered in service in 1989; it's powered by two turboprop engine and it's used typically as a regional airliner. The main purpose of its design was to increase the seating capacity throughout the stretching of the fuselage by 4.5m, an increased wingspan, more powerful engines and an increased fuel capacity by approximately 10%.

The Boeing 747 is a wide-body commercial jet airliner and cargo aircraft, often referred to by its original nickname, Jumbo Jet, or Queen of the Skies. Its distinctive hump upper deck along the forward part of the aircraft makes it among the world's most recognizable aircraft, and it was the first wide-body produced. Manufactured by Boeing's Commercial Airplane unit in the United States, the original version of the 747 had two and a half times greater capacity than the Boeing 707, one of the common large commercial aircraft of the 1960s. The four-engine 747 uses a double deck configuration for part of its length and it's available in passenger and other versions. Boeing designed the 747's hump-like upper deck to serve as a first class lounge or extra seating, and to allow the aircraft to be easily converted to a cargo carrier by removing seats and installing a front cargo door. The 747-100B model was developed from the 747-100SR, using its stronger airframe and landing gear design; the type had an increased fuel capacity of 182000 L, allowing for a 5000 nautical mile range with a typical 452 passengers payload, and an increased maximum take-off weight of 340000 kg was offered; unlike the original 747-100, the 747-100B was offered with Pratt & Whitney JT9D-7A, General Electric CF6-50, or Rolls-Royce RB211-524 turbofan engines.

The two presented tests share the same architecture so that a general guideline can be followed; this strategy has been designed with the purpose of making a general procedure in order to simplify user's work.

For more clarity, listings of the two test types are reported, as an exemplificative practice, only in the case of the ATR-72 turboprop aircraft.

First of all it's necessary to set up all default folders in order to make them achievable from any location inside the software; this is done with the static method `initWorkingDirectoryTree` of the `MyConfiguration` class located in `JPADConfigs` package. In this way, every time the user wants to point at a specific folder, like the input or output directory, it's necessary only to call the static method `getDir`, also from `MyConfiguration` class, which reads the folder name, from a dedicated enumeration, and associate it with the related directory from a `HashMap` named `mapPaths`.

The second step is to read the engine and the fuel fractions databases with the related java class reader; this particular class type uses the super class `DatabaseReader`, which implements the use of `MyHDFReader` class, to access an .h5 dataset values. For more information about how to build and use an HDF database, see Appendix A.

```

1 public class PayloadRange_Test_TP{
2     //-----
3     // MAIN:
4     public static void main(String[] args) throws
5             HDF5LibraryException, NullPointerException{
6         System.out.println("-----");
7         System.out.println("PayloadRangeCalc_Test :: main");
8         System.out.println("-----");
9         //-----
10        // Assign all default folders
11        MyConfiguration.initWorkingDirectoryTree();
12        //-----
13        // Setup database(s)
14        String databaseFolderPath = MyConfiguration.getDir(FoldersEnum.DATABASE_DIR);
15        String aerodynamicDatabaseFileName = "Aerodynamic_Database_Ultimate.h5";
16        String fuelFractionDatabaseFileName = "FuelFractions.h5";
17        AerodynamicDatabaseReader aeroDatabaseReader = new AerodynamicDatabaseReader(
18            databaseFolderPath,
19            aerodynamicDatabaseFileName
20        );
21        FuelFractionDatabaseReader fuelFractionReader = new FuelFractionDatabaseReader(
22            databaseFolderPath,
23            fuelFractionDatabaseFileName
24        );

```

Listing 2.1 Excerpt of the ATR-72 Payload-Range test - preliminary steps

Now that all required resources are set up, following steps are to create the aircraft model, assign its operating conditions and perform all necessary analysis like the aerodynamic one. This is done throughout the use of the following three fundamental classes, which modes of operation are explained in the flowchart of figure 3.5.

- Aircraft class
- OperatingConditions class
- ACAnalysisManager class

```

1 //-----
2 // Operating Condition / Aircraft / AnalysisManager
3 // (geometry calculations)
4 OperatingConditions theCondition = new OperatingConditions();
5
6 Aircraft aircraft = Aircraft.createDefaultAircraft("ATR-72");
7
8 aircraft.get_theAerodynamics().set_aerodynamicDatabaseReader(aeroDatabaseReader);
9 aircraft.get_theFuelTank().setFuelFractionDatabase(fuelFractionReader);
10 aircraft.set_name("ATR-72");
11 aircraft.get_wing().set_theCurrentAirfoil(new MyAirfoil(
12     aircraft.get_wing(),
13     0.5)
14 );
15
16 ACAnalysisManager theAnalysis = new ACAnalysisManager(theCondition);
17 theAnalysis.updateGeometry(aircraft);
18
19 //-----
20 // Set the CoG(Bypass the Balance analysis allowing
21 // to perform Aerodynamic analysis only)
22 CenterOfGravity cgMTOM = new CenterOfGravity();
23
24 // x_cg in body-ref.-frame
25 cgMTOM.set_xBRF(Amount.valueOf(12.0, SI.METER));
26 cgMTOM.set_yBRF(Amount.valueOf(0.0, SI.METER));
27 cgMTOM.set_zBRF(Amount.valueOf(2.3, SI.METER));
28
29 aircraft.get_theBalance().set_cgMTOM(cgMTOM);
30 aircraft.get_HTail().calculateArms(aircraft);
31 aircraft.get_VTail().calculateArms(aircraft);
32 theAnalysis.doAnalysis(aircraft, AnalysisTypeEnum.AERODYNAMIC);

```

Listing 2.2 Excerpt of the ATR-72 Payload-Range test - Aircraft, OperatingConditions and ACAnalysisManager setup

All data required by the `PayloadRangeCalc` class are now ready to be used and it's possible to create an instance of this class accessing, in this way, to all its methods, which have been explained in the previous paragraph.

```

1 //-----
2 // Creating the Calculator Object
3 PayloadRangeCalc test = new PayloadRangeCalc(
4     theCondition,
5     aircraft,
6     AirplaneType.TURBOPROP_REGIONAL
7 );

```

Listing 2.3 Excerpt of the ATR-72 Payload-Range test - Payload-Range class instance creation

The first check that is implemented has the purpose of inspect whether or not the chosen cruise Mach number is bigger than the crest critical one; in this case a warning message is launched in order to inform the user of the situation. The method demanded of this is `checkCriticalMach` which accepts in input a given Mach number, compares it with the one calculated with Kroo method [5], starting from the cruise lift coefficient, and return a boolean variable that is true only if the chosen Mach number is bigger than the crest critical one indeed.

```

1  // -----CRITICAL MACH NUMBER CHECK-----
2  boolean check = test.checkCriticalMach(theCondition.get_machCurrent() );
3
4  if (check)
5      System.out.println("\n-----"
6      +"\nCurrent Mach lower then critical Mach number"
7      +"Current Mach = " + theCondition.get_machCurrent()
8      +"Critical Mach = " + test.getCriticalMach()
9      +"\\n\\t CHECK PASSED -> PROCEDING TO CALCULATION "
10     +"\\n\\n"
11     +"-----");
12 else{
13     System.err.println("\n-----"
14     +"\nCurrent Mach bigger then critical Mach number"
15     +"Current Mach = " + theCondition.get_machCurrent()
16     +"Critical Mach = " + test.getCriticalMach()
17     +"\\n\\t CHECK NOT PASSED -> WARNING!!! "
18     +"\\n\\n"
19     +"-----");
20 }
```

Listing 2.4 Excerpt of the ATR-72 Payload-Range test - critical Mach number check

```

1 -----
2 Current Mach is lower then critical Mach number.
3 Current Mach = 0.43
4 Critical Mach = 0.6659791543529567
5
6 CHECK PASSED --> PROCEDING TO CALCULATION
7 -----
```

Listing 2.5 Excerpt of the ATR-72 Payload-Range test results - critical Mach number check

```

1 -----
2 Current Mach is lower then critical Mach number.
3 Current Mach = 0.84
4 Critical Mach = 0.8490814607347361
5
6 CHECK PASSED --> PROCEDING TO CALCULATION
7 -----
```

Listing 2.6 Excerpt of the B747-100B Payload-Range test results - critical Mach number check

At this point, if the user wants to compare the chosen Mach number condition with the best range one, all that it's needed is to invoke the `createRangeArray` method, for both the operative conditions, and the `createPayloadArray` one; after that the diagram is generated from the method `createPayloadRangeCharts_Mach`.

```

1  // -----BEST RANGE CASE-----
2  System.out.println();
3  System.out.println("-----BEST RANGE CASE-----");
4  List<Amount<Length>> vRange_BR = test
5      .createRangeArray(
6          test.getMaxTakeOffMass(),
7          test.getSweepHalfChordEquivalent(),
8          test.getSurface(),
9          test.getCd0(),
10         test.getOswald(),
11         aircraft.get_theAerodynamics().getcLE(),
12         test.getAr(),
13         test.getTcMax(),
14         test.setByPassRatio(0.0),
15         test.getEta(),
16         test.getAltitude(),
17         test.calculateBestRangeMach(
18             EngineTypeEnum.TURBOPROP,
19             test.getSurface(),
20             test.getAr(),
21             test.getOswald(),
22             test.getCd0(),
23             test.getAltitude()),
24             true);
25 // -----USER CURRENT MACH-----
26 System.out.println();
27 System.out.println("-----CURRENT MACH CASE-----");
28 List<Amount<Length>> vRange_CM = test
29     .createRangeArray(
30         test.getMaxTakeOffMass(),
31         test.getSweepHalfChordEquivalent(),
32         test.getSurface(),
33         test.getCd0(),
34         test.getOswald(),
35         test.getCl(),
36         test.getAr(),
37         test.getTcMax(),
38         test.setByPassRatio(0.0),
39         test.getEta(),
40         test.getAltitude(),
41         test.getCurrentMach(),
42         false);
43 // -----PLOTTING-----
44 // Mach parameterization:
45 List<Double> vPayload = test.createPayloadArray();
46 test.createPayloadRangeCharts_Mach(
47     vRange_BR,
```

```

48         vRange_CM,
49         vPayload,
50         test.calculateBestRangeMach(
51             EngineTypeEnum.TURBOPROP,
52             test.getSurface(),
53             test.getAr(),
54             test.getOswald(),
55             test.getCd0(),
56             test.getAltitude(),
57             test.getCurrentMach());
58     }
59 //-----
60 // END OF THE TEST
61 }
```

Listing 2.7 Excerpt of the ATR-72 Payload-Range test - Payload-Range diagram evaluation and plot

Otherwise, if it's the maximum take-off mass parameterization the wanted analysis, the required call is for `createPayloadRangeMatrices` method followed by the plotting method `createPayloadRangeCharts_MaxTakeOffMass`.

```

1  // -----MTOM PARAMETERIZATION-----
2  test.createPayloadRangeMatrices(
3      test.getSweepHalfChordEquivalent(),
4      test.getSurface(),
5      test.getCd0(),
6      test.getOswald(),
7      test.getCl(),
8      test.getAr(),
9      test.getTcMax(),
10     test.setByPassRatio(0.0),
11     test.getEta(),
12     test.getAltitude(),
13     test.getCurrentMach(),
14     false
15 );
16 // -----PLOTTING-----
17 // MTOM parameterization:
18 test.createPayloadRangeCharts_MaxTakeOffMass(
19     test.getRangeMatrix(),
20     test.getPayloadMatrix()
21 );
22 }
23 }
```

Listing 2.8 Excerpt of the ATR-72 Payload-Range test - maximum take-off mass parameterization

In conclusion, following pages shows a summary of input data used for each analyzed aircraft, together with their related results in terms of Payload-Range diagrams for both the chosen Mach number and best range comparison and max take-off mass parameterization.

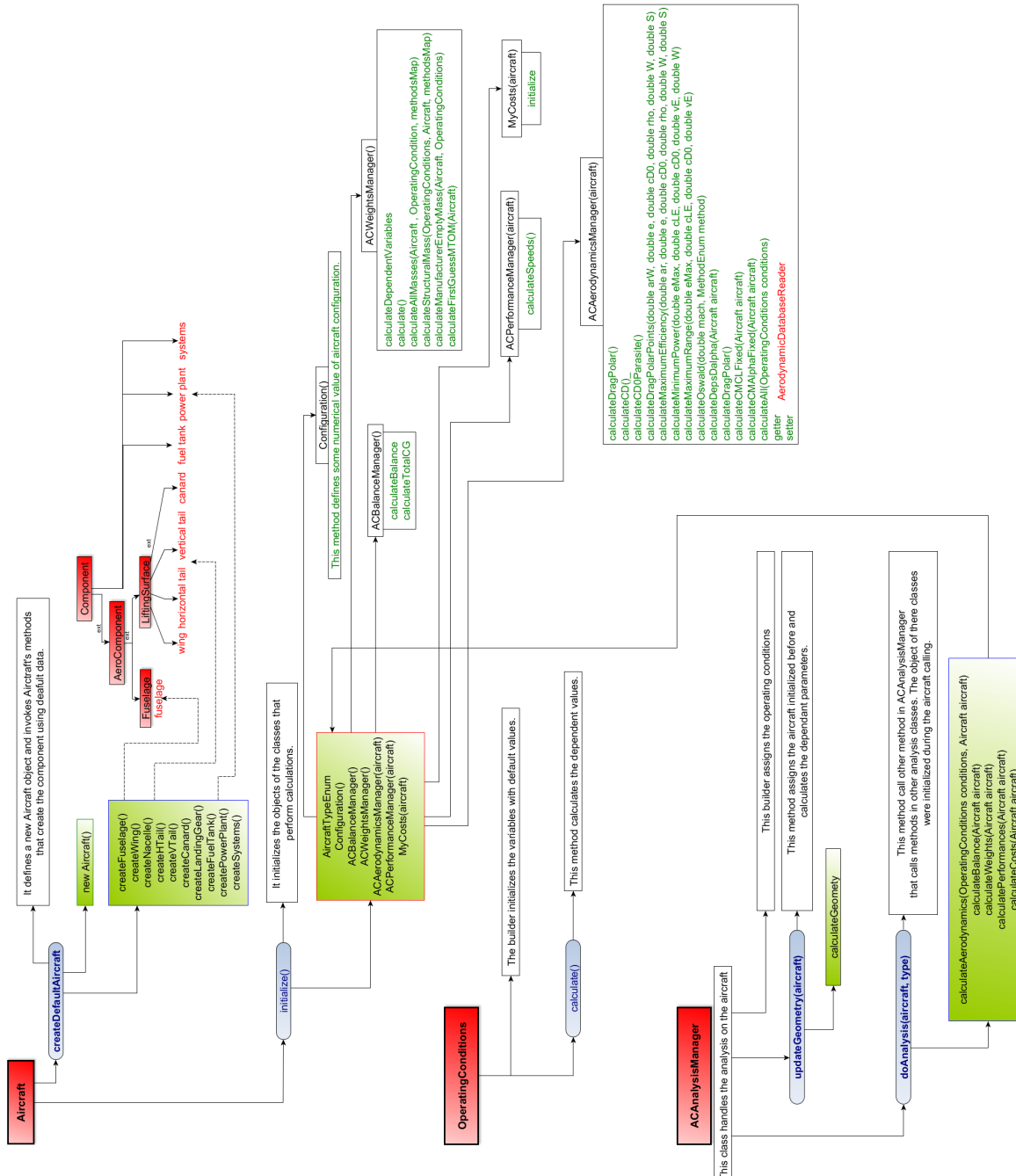


Figure 2.5 Aircraft, OperatingConditions and ACAnalysisManager flowchart

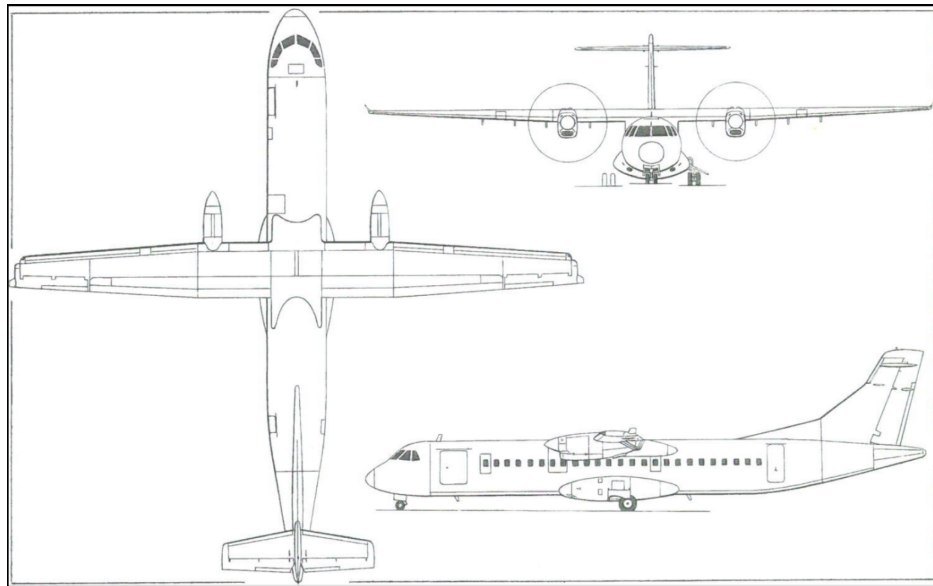


Figure 2.6 ATR-72 views – Jane's All the World's Aircraft 2004-2005

Variables	Description	Values
altitude	Cruise altitude	6000 m
machCurrent	The user chosen Mach number	0,43
surface	Wing surface	61 m ²
taperRatioEquivalent	Taper ratio of the equivalent wing	0,545
maxTakeOffMass	maximum take-off mass	23063,579 kg
operatingEmptyMass	operating empty mass	12935,579 kg
maxFuelMass	maximum fuel mass	5000,000 kg
nPassMax	maximum number of passengers	72
sweepLEEEquivalent	Equivalent wing leading edge sweep angle	3,142 °
oswald	Wing oswald factor	0,7585
byPassRatio	Engine bypass ratio	0,0
eta	propeller efficiency	0,85
tcMax	Mean maximum thickness of the wing	0,1675
cl	The cruise lift coefficient	0,45
ar	Wing aspect ratio	12
cd0	Wing parasite drag coefficient	0,0317

Table 2.4 ATR-72 input data

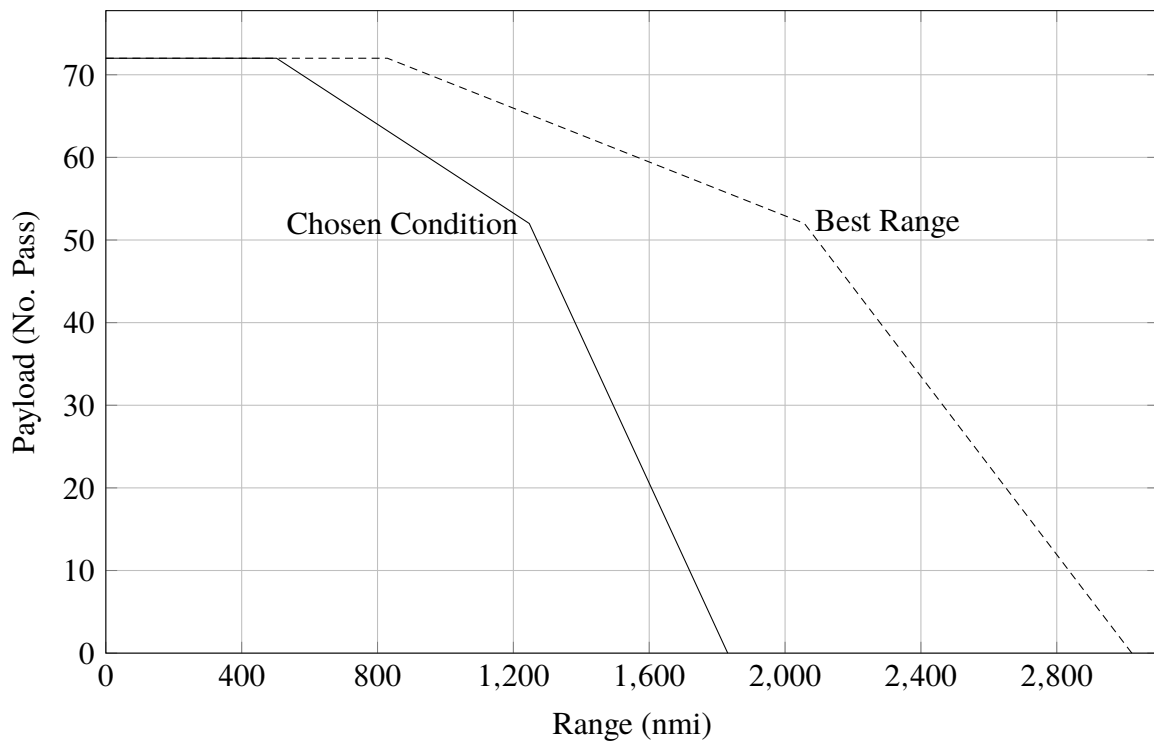


Figure 2.7 ATR-72 Payload-Range - Chosen Mach number and best range comparison

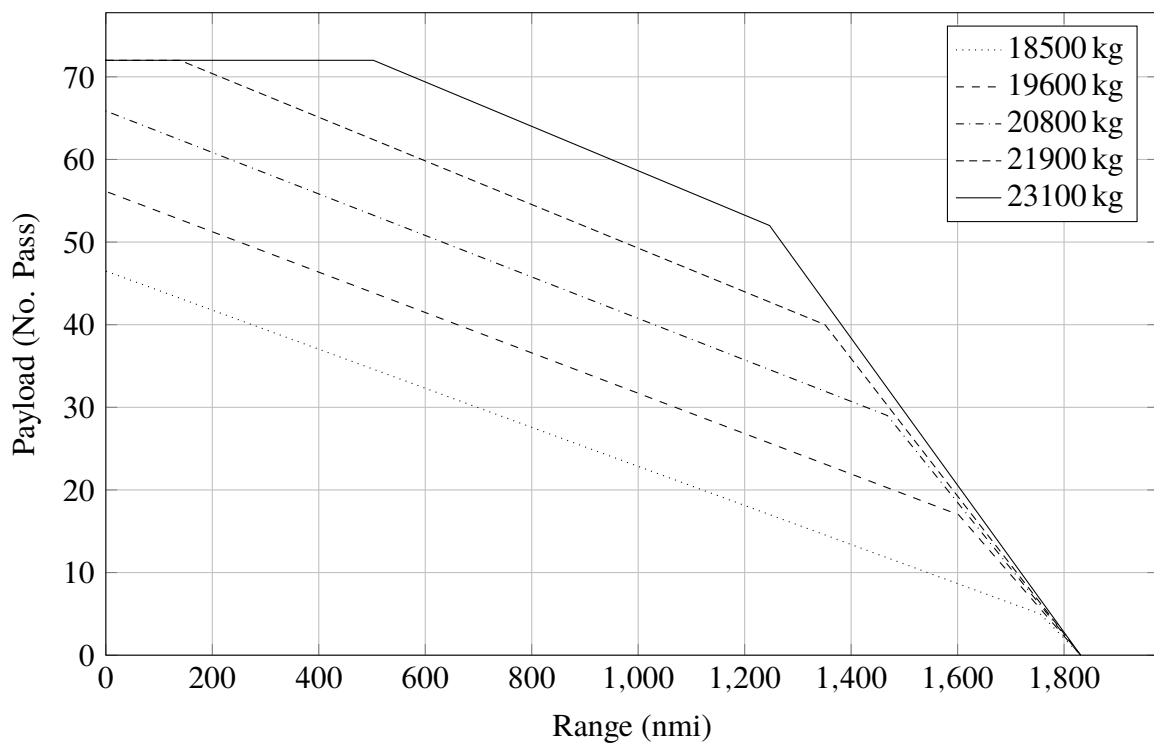


Figure 2.8 ATR-72 Payload-Range - Maximum take-off mass parameterization

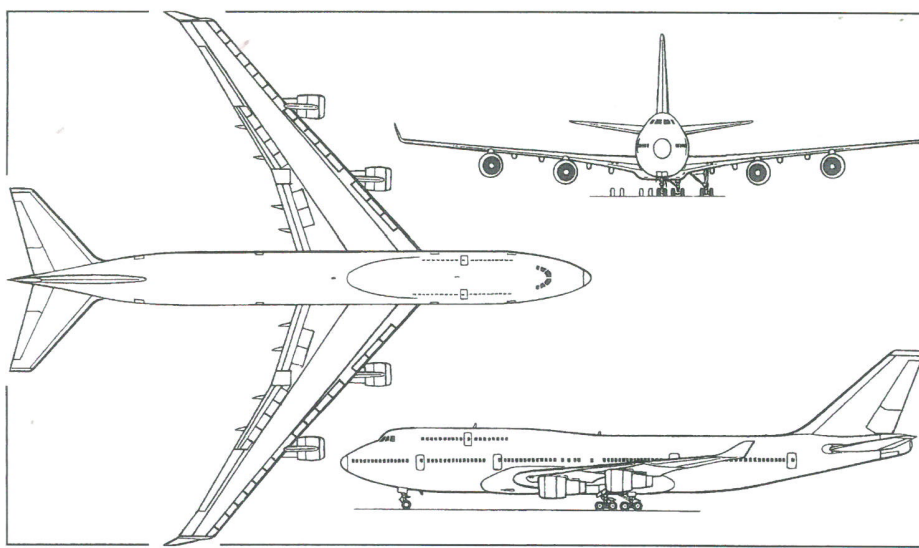


Figure 2.9 B747-100B views – Jane's All the World's Aircraft 2004-2005

Variables	Description	Values
altitude	Cruise altitude	11000 m
machCurrent	The user chosen Mach number	0,83
surface	Wing surface	511 m ²
taperRatioEquivalent	Taper ratio of the equivalent wing	0,284
maxTakeOffMass	maximum take-off mass	354991,506 kg
operatingEmptyMass	operating empty mass	153131,986 kg
maxFuelMass	maximum fuel mass	147409,520 kg
nPassMax	maximum number of passengers	550
sweepLEEEquivalent	Equivalent wing leading edge sweep angle	38,429 °
oswald	Wing oswald factor	0,6277
byPassRatio	Engine bypass ratio	5,0
eta	propeller efficiency	0,0
tcMax	Mean maximum thickness of the wing	0,1292
cl	The cruise lift coefficient	0,45
ar	Wing aspect ratio	6,9
cd0	Wing parasite drag coefficient	0,0182

Table 2.5 B747-100B input data

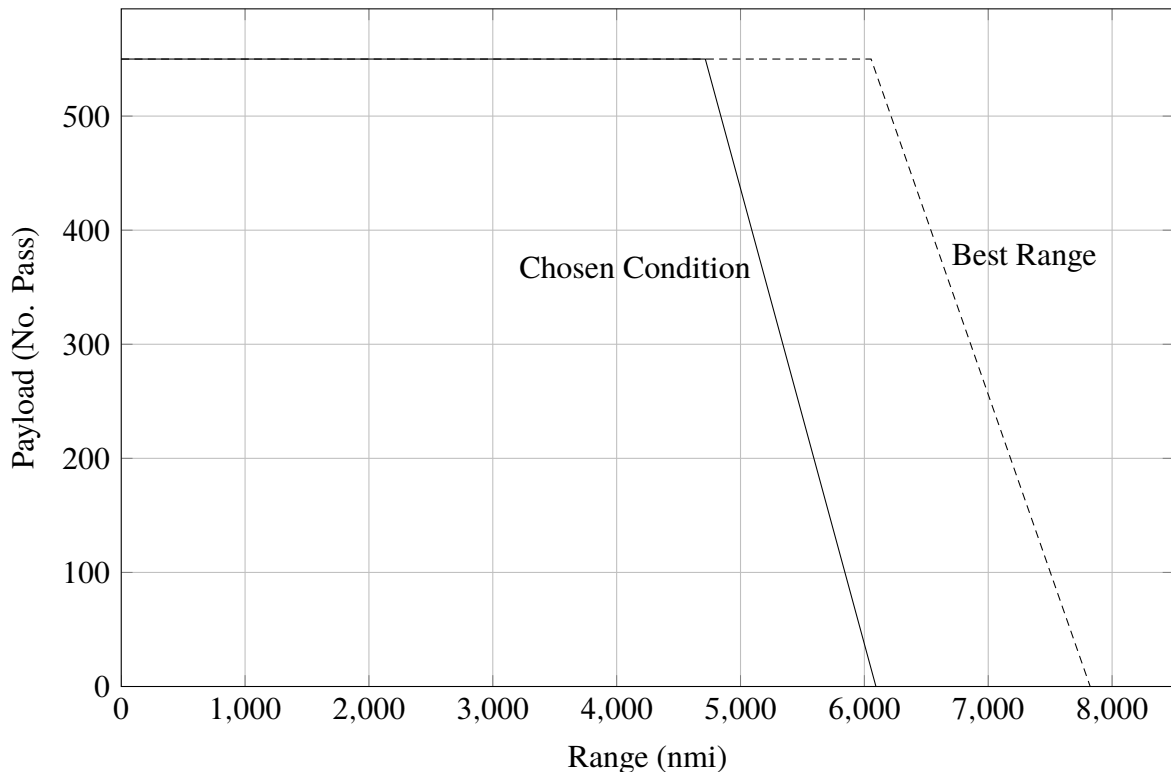


Figure 2.10 B747-100B Payload-Range - Chosen Mach number and best range comparison

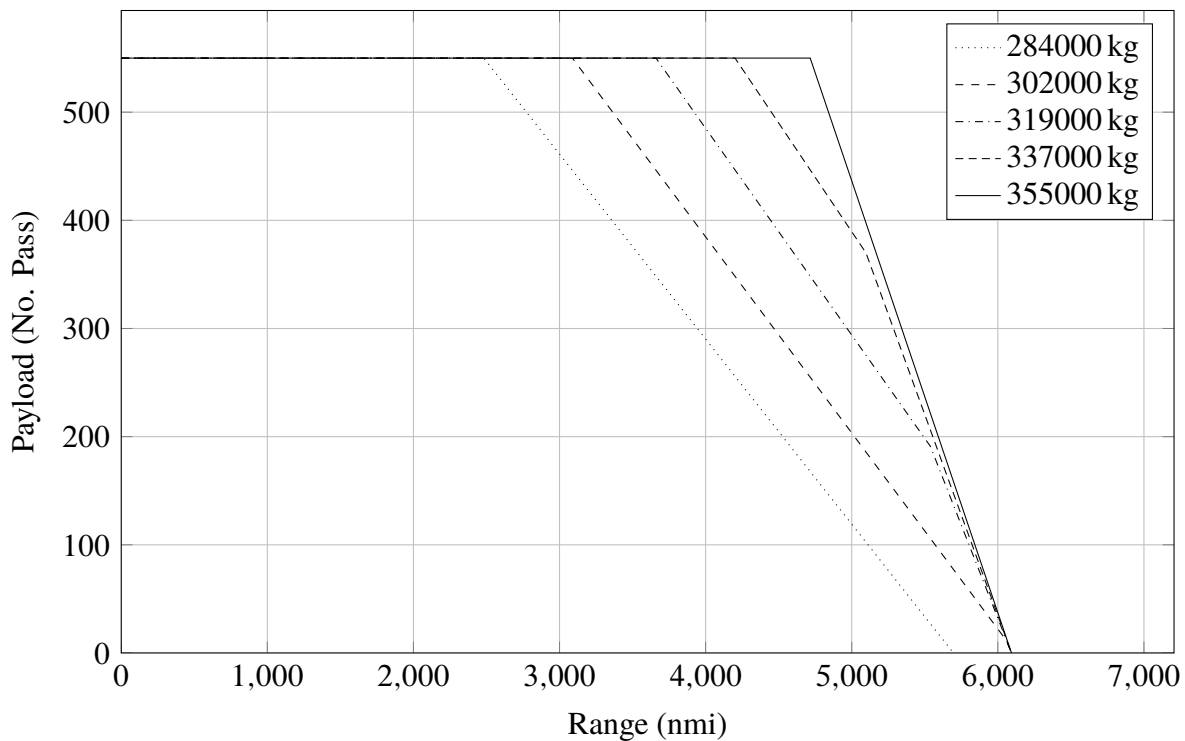


Figure 2.11 B747-100B Payload-Range - Maximum take-off mass parameterization

Variables	Values	Variables	Values
Range (point A)	0 nmi	Range (point A)	0 nmi
Payload (point A)	72 passengers	Payload (point A)	550 passengers
Range (point B)	502.587 nmi	Range (point B)	4714.449 nmi
Payload (point B)	72 passengers	Payload (point B)	550 passengers
Range (point C)	1246.827 nmi	Range (point C)	4715.799 nmi
Payload (point C)	52 passengers	Payload (point C)	550 passengers
Range (point D)	1831.171 nmi	Range (point D)	6093.423 nmi
Payload (point D)	0 passengers	Payload (point D)	0 passengers
C_L	0.421	C_L	0.385
C_D	0.0388	C_D	0.0296
Efficiency	10.853	Efficiency	13.00518
SFC	0.424	SFC	0.626

Table 2.6 Review of ATR-72 (left) and B747-100B (right) results at chosen Mach number conditions

Chapter 3

SPECIFIC RANGE AND CRUISE GRID

In this chapter an analysis of the specific range is performed with the aim of obtain useful information about cruise performance.

In particular, starting from generalized performance evaluation and interfacing them with the fuel consumption, the final objective will be to define the specific range as function of Mach number, obtaining the so called *cruise grid chart* which is a very important tool for pilots because it allows to choose the correct speed, during cruising phase, in order to follow some mission objectives like minimum fuel consumption or a fast cruise.

3.1 Theoretical background

The first step that has to be done in order to obtain the *cruise grid chart* is to define generalized performance in terms of thrust and drag. The *generalized* attribute given to these quantities stands for the fact that they are independents from altitude and this result is reached through the parameter δ which represents a ratio between the total pressure at compressor inlet and the standard pressure at sea level.

Regarding the thrust, the generalized version can be obtained by dividing it by δ as shown below.

$$\frac{T}{\delta} = \frac{T_f}{\delta} - M \cdot a_0 \cdot \frac{\sqrt{\theta \cdot m_a}}{\delta} \quad (3.1)$$

where

- T , is the net thrust
- T_f , is the gross thrust
- M , is the mach number
- a_0 , is the sound speed at sea level

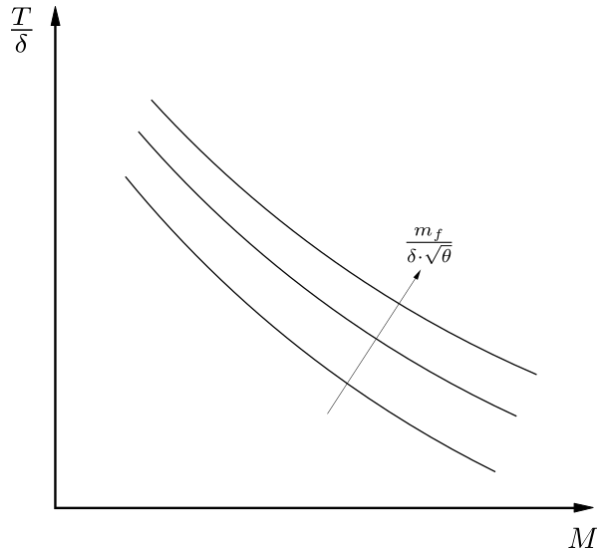


Figure 3.1 Qualitative trend of the generalized thrust v.s. Mach number parameterized in generalized fuel flow rate

- $\frac{\sqrt{\theta} \cdot m_a}{\delta}$, is the generalized air flow rate which is function of the generalized fuel flow rate given by $\frac{m_f}{\delta \cdot \sqrt{\theta}}$

so that the generalized thrust results as a function of Mach number and generalized fuel flow rate.

$$\frac{T}{\delta} = \frac{T_f}{\delta} \cdot f \left(\frac{m_f}{\delta \cdot \sqrt{\theta}} \right) \quad (3.2)$$

As shown in figure 3.1 the generalized thrust decreases with Mach number, at given fuel flow rate, and grows with the latter, at given Mach number. This because if the Mach number grows at fixed fuel flow rate, the air flow rate grows reducing the thrust; otherwise, if fuel flow rate grows at fixed Mach number, air flow rate is lower giving more thrust.

With this function it's possible to correlate generalized thrust to hourly fuel consumption which is a main keypoint in building the cruise grid chart of an endurance based aircraft such as UAV.

Since transport aircrafts rely more on range performance, it's necessary to obtain the same relationship between generalized thrust and fuel consumption referred to the generalized specific range indicated with $\delta \bar{s}$.

Dividing the generalized fuel flow rate, which is dimensionally equal to $\frac{\text{kg}}{\text{s}}$, by a velocity, the result has a dimension of $\frac{\text{m}}{\text{kg}}$ that represents the reciprocal of the specific range. In this way it's possible to state the following relation.

$$\frac{m_f}{\delta \cdot \sqrt{\theta}} = \frac{M \cdot a_0}{\delta \bar{s}} \quad (3.3)$$

As expected from the relation (3.3) the thrust has a trend which is the inverse of the previous parameterization. In fact now, for a given Mach number, if the pilot wants to go farther he has

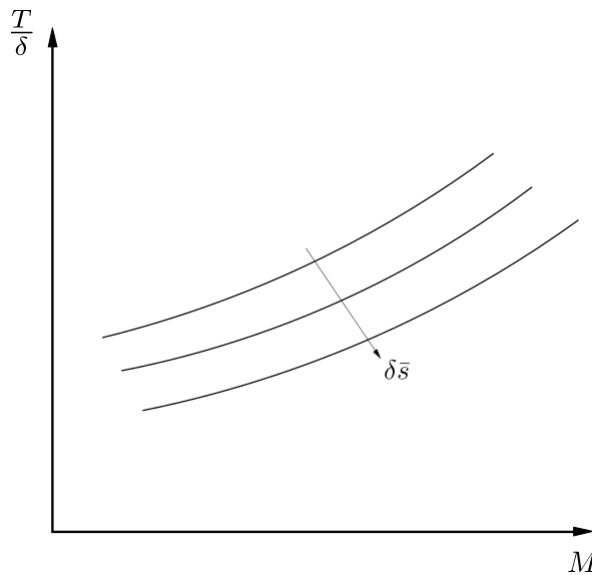


Figure 3.2 Qualitative trend of the generalized thrust v.s. Mach number parameterized in generalized specific range

to decrease the thrust in order to reduce the fuel consumption; otherwise, at a given distance to reach, the pilot has to increase the thrust in order to make the Mach number grows.

Since the thrust has always to be compared with the drag in order to evaluate if the aircraft can fly in a specific cruise condition without loosing speed and altitude, it's necessary to obtain a generalized drag trend as well.

This is very similar to the drag trend, as can be seen from figure 3.3, and it depends from aircraft weight as well; but, since these have to be generalized quantities, the weight is a generalized weight too.

By the overlap of figure 3.2 and figure 3.3 charts, it's easy to note that the best Mach number, for a given generalized weight, is located at the intersection of the two curves as reported in figure 3.4. In fact, in order to obtain a bigger specific range at fixed weight, the generalized

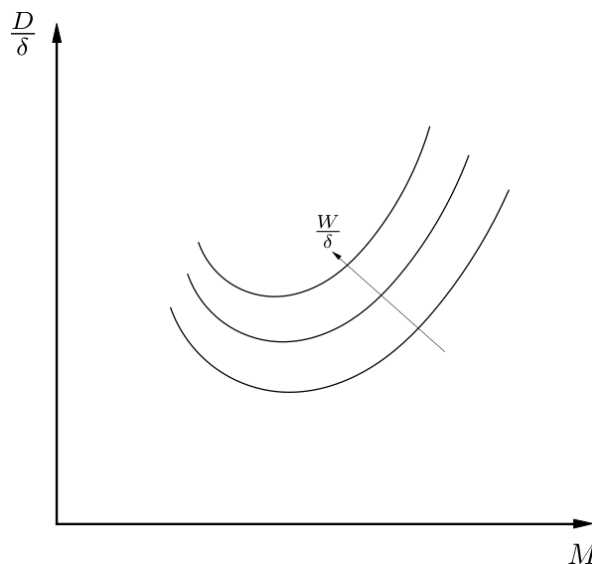


Figure 3.3 Qualitative trend of the generalized drag v.s. Mach number parameterized in generalized weight

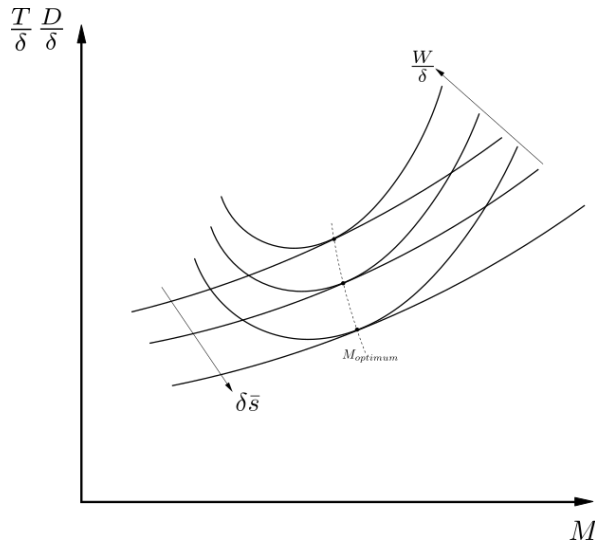


Figure 3.4 Comparison between generalized drag and generalized thrust as functions of Mach number

drag would be higher than the generalized thrust; otherwise, if the pilot wants to fly faster at given weight, he has to increase thrust so that the specific range will decrease due to the increasing fuel consumption.

Since during the cruise phase the aircraft weight decreases continuously, the pilot has to gain altitude in order to leave the generalized weight unchanged; this explains why during cruise the aircraft continues to climb.

The specific range can also be connected to Breguet formulas (2.1) as it can be obtained by dividing the autonomy factor, *A.F.*, by the aircraft weight; in particular the autonomy factor, groups three main aircraft efficiency and can be written as follow.

$$A.F. = \frac{\eta_p}{SFC} \cdot \left(\frac{L}{D} \right) \quad \text{if propeller engine driven} \quad (3.4a)$$

$$A.F. = \frac{V}{SFCJ} \cdot \left(\frac{L}{D} \right) \quad \text{if jet engine driven} \quad (3.4b)$$

where

- η_p , is propeller efficiency
- SFC , is related to propulsive efficiency
- $\left(\frac{L}{D} \right)$, is the aerodynamic efficiency

At given generalized weight and generalized specific range, the optimum Mach is known as explained before and so the autonomy factor can be calculated by multiplying $\frac{W}{\delta}$ and $\delta s̄$. Repeating this operation for different generalized weight conditions, allows to define the autonomy factor trend as function of the generalized weight in which each point of the chart is related to an optimum Mach number for the specific range.

As can be seen from figure 3.5 the autonomy factor has a maximum at a specific generalized weight which is the one that the pilot should maintain during the cruise phase.

If the altitude is fixed, and so δ is constant, the chart in figure 3.5 can be seen as function of Mach number for a given aircraft weight; at this point, knowing that the autonomy factor

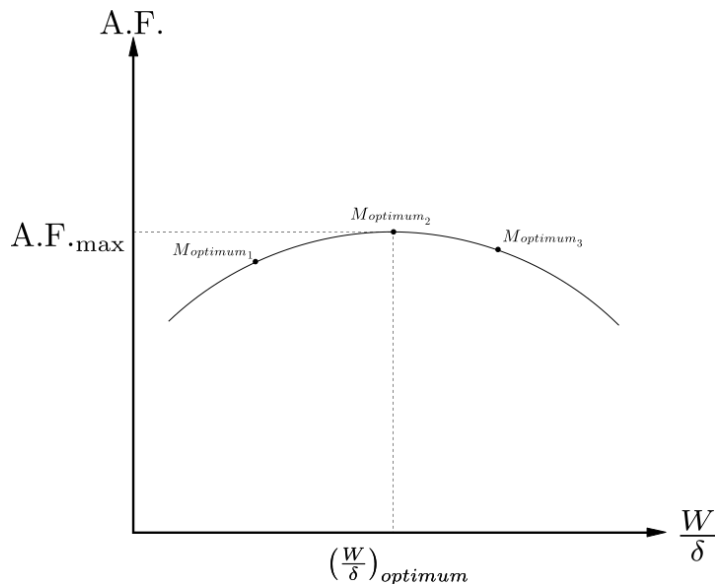


Figure 3.5 Autonomy factor trend as function of the generalized weight

leads to the specific range if divided by the aircraft weight, it's possible to define the specific range trend as function of the Mach number parameterized in aircraft weight.

The chart, so obtained, in figure 3.6 is the one upon which the cruise grid is defined; on the latter, in fact, four lines are drawn each of which is related to a precise mission objective.

It's important to highlight that, on long distances, the maximum distance line is not often followed during the cruise because it is tied to a low speed which adversely affects the total flight time increasing the D.O.C.; in order to avoid this condition, pilots prefer to follow the long range line which has only 1% of penalty on the specific range but, at the same time, allows to fly at significantly higher speed with benefits on flight time and, as a result, on the D.O.C.

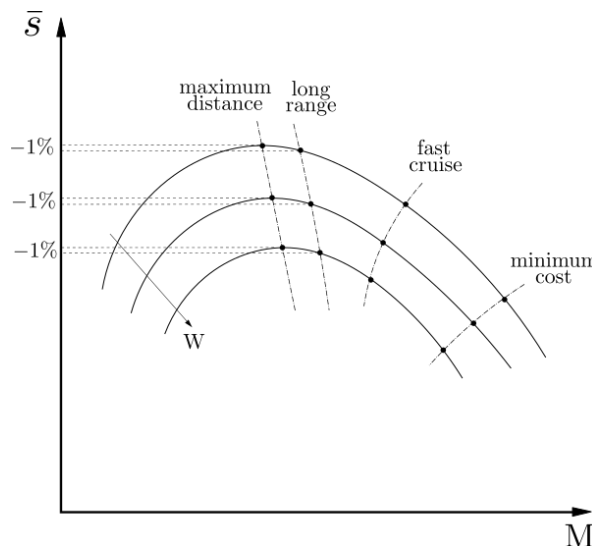


Figure 3.6 Specific range as function of the Mach number parameterized in aircraft weight

3.2 Java class architecture

After having introduced the theory behind the cruise grid chart, a presentation of the related Java class inside JPAD is shown. Using the same philosophy of the previous chapter, a dedicated class, named `SpecificRangeCalc`, has been implemented inside which a series of static methods provide the needed calculation tools. Generally speaking, the guideline followed in creating this class is to assign an array of Mach numbers, starting from the one relative to the minimum cruising speed and ending with the maximum cruising speed at that altitude and weight, and then evaluate the *SFC*, from engine database, for each Mach number; from here the *A.F.* is built after the evaluation of the aerodynamic efficiency for each value of the same Mach array. Finally the specific range is calculated, in $\frac{\text{nmi}}{\text{lbs}}$, dividing the *A.F.* by the aircraft max take off mass.

The first static method presented is `calculateEfficiencyVsMach`. It allows to evaluate the aerodynamic efficiency value for each Mach number of a given array through the evaluation of the C_L and the relative C_D from the aircraft total drag polar; in particular the two aerodynamic coefficients are calculated by calling other two static methods which come from two classes of the aerodynamic calculator package of `JPADCore` named, respectively, `LiftCalc` and `DragCalc`.

The static `LiftCalc` method, named `calculateLiftCoeff`, performs the C_L calculation using the following formula, valid in cruise phase.

$$C_L = \frac{2W}{\rho SV^2} \quad (3.5)$$

where V , is the TAS speed derived from the actual Mach number of the array at that the given altitude.

On the other hand, the static `DragCalc` method, named `calculateCDTotal`, performs the C_D calculation using the total drag polar expression.

$$C_D = C_{D0} + \frac{C_L^2}{\pi ARe} + C_{D\text{wave}} \quad (3.6)$$

<code>maxTakeOffMass</code>	Maximum take-off mass
<code>sweepHalfChordEquivalent</code>	Equivalent wing sweep angle at half chord
<code>surface</code>	Wing surface
<code>cd0</code>	Wing c_{D0}
<code>oswald</code>	Wing oswald factor
<code>mach</code>	An array of Mach numbers
<code>ar</code>	Wing aspect ratio
<code>tcMax</code>	Mean maximum thickness of the wing
<code>altitude</code>	Cruise altitude
<code>airfoilType</code>	The wing airfoil type from the related <code>AirfoilType</code> enumeration

Table 3.1 `calculateEfficiencyVsMach` input data

mach	An array of Mach numbers
altitude	Cruise altitude
bpr	Engine By-Pass ratio
engineType	The engine type from the related <code>EngineType</code> enumeration

Table 3.2 `calculateSfcVsMach` input data

where the $C_{D\text{wave}}$ is calculated as presented in [11].

The second static method implemented is `calculateSfcVsMach`, which accepts as input data reported in table 3.2 allows to evaluate the *SFC* of a turboprop aircraft, or the *SFCJ* of a turbofan aircraft, for each Mach number of the given array by reading data from the related engine database.

Finally, the two previous method leads to the last one named `calculateSpecificRangeVsMach` which allows to calculate the *A.F.* and, from it, the specific range by implementing the (3.4a) or the (3.4b) depending on the given engine type.

To do this, it's necessary to give as input the Mach numbers array, the aerodynamic efficiency array calculated with `calculateEfficiencyVsMach` and the *SFC* array calculated with `calculateSfcVsMach` as shown in table 3.3.

The class is completed by other four static methods demanded of plotting the results; in particular, using the same approach shown in the previous chapter, a .png and a .tikz output images are created for each of the *SFC*, the aerodynamic efficiency and the specific range.

It's important to highlight that the first of these plotting methods, which is named `createSpecificRangeChart` and is demanded of plotting the cruise grid chart, has implemented, inside it, the evaluation of the maximum range condition as well as the long range one; this by calculating all maximum points and, from them, all points at -1% of penalty obtained through the evaluation of the bigger of the two intersection points that the line at -1% of penalty defines on each specific range curve.

maxTakeOffMass	Maximum take-off mass
mach	An array of Mach numbers
efficiency	An array of aerodynamic efficiency values
sfc	An array of SFC values
bpr	Engine By-Pass ratio
altitude	Cruise altitude
eta	Propeller efficiency (set to zero in case of turbofan)
engineType	The engine type from the related <code>EngineType</code> enumeration

Table 3.3 `calculateSpecificRangeVsMach` input data

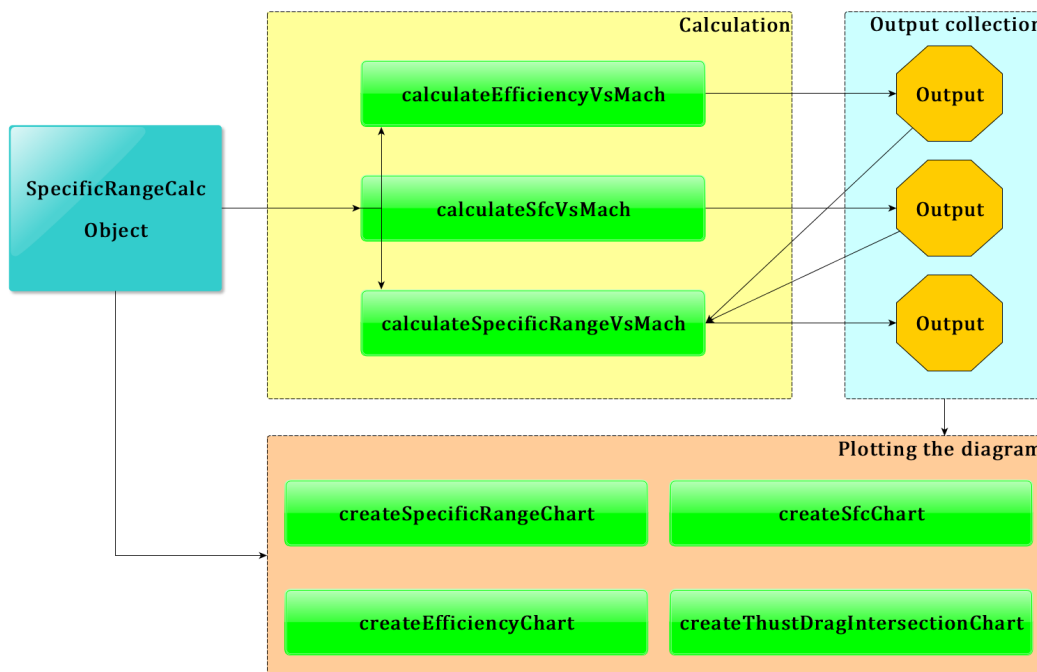


Figure 3.7 SpecificRangeCalc class flowchart

The fourth method is, instead, used for plotting the intersection between the required and available thrust, giving as input a speed array, the altitude and two `List` of `custom Map` named `DragMap` and `ThrustMap`; these are two classes used to store all data related to drag and thrust curves like the aircraft weight, the current altitude, the speed array on which the drag or thrust are evaluated and, finally, the drag or thrust array itself.

In conclusion a flowchart of the described class is shown in figure 3.7 in order to simplify its understanding.

3.3 Case study: ATR-72 and B747-100B

In order to validate all the theoretical concepts explained in the previous paragraphs, as well as to give to the reader a useful example of how to handle this class usage, the following pages shows two application of the class methods made upon the two default aircraft described in paragraph 1.4.

Once all preliminary steps have been completed, as explained in paragraph 1.4, it's possible to start the test of this class.

First of all, since the cruise grid chart is parameterized in aircraft weight, an array of aircraft masses has to be created; in particular, in this test, a variation of mass of -10% has been implemented, starting from the aircraft maximum take-off mass until it reaches the 60% of the latter.

The second step is to define the independent variable, which is the Mach number, and in particular it's necessary to identify the upper and lower limitations of its array; this can be done by evaluating the required thrust, which is equal to the drag during cruise, and comparing it with the available thrust supplied by the power plant.

```

1   double[] maxTakeOffMassArray = new double[5];
2   for (int i=0; i<5; i++)
3       maxTakeOffMassArray[i] = aircraft.get_weights().get_MTOM()
4           .plus(aircraft.get_weights().get_MLM())
5           .divide(2)
6           .getEstimatedValue()
7           *(1-0.1*(4-i));
8
9   double[] weight = new double[maxTakeOffMassArray.length];
10  for(int i=0; i<weight.length; i++)
11      weight[i] = maxTakeOffMassArray[i]*AtmosphereCalc.g0.getEstimatedValue();

```

Listing 3.1 Mass variation in Specific Range test - B747-100B

By the intersections of the latter, the two required speeds can be derived; otherwise, if the minimum speed intersection can't be found, the cruising stalling speed, at that weight and altitude condition and for a specified $c_{L_{max}}$, replaces the missing intersection abscissa.

In terms of code, the last step can be carried out using the static method, of the JPADCore class `PerformanceCalcUtils`, named `calculateDragThrustIntersection`; the latter requires as input the following data:

- An array of altitudes
- An array of speeds
- An array of weights
- An array of throttle settings
- An array of flight conditions chosen from the `EngineOperatingConditionEnum` enumeration
- The engine by-pass ratio, set to zero in case of propeller aircraft
- The wing surface
- Wing $C_{L_{max}}$ in clean configuration
- A List of custom data map named `DragMap`
- A List of custom data map named `ThrustMap`

The last two input are two collections of maps designed to store all data necessary to manage curves of drag, or thrust, as function of speed; in particular, in the reported example, the drag and thrust arrays passed to each of them are calculated using the static method of the JPADCore classes `DragCalc` and `ThrustCalc` named, respectively, `calculateDragVsSpeed` and `calculateThrustVsSpeed`.

The first one implements the classic formula of drag as function of speed and of the c_D calculated with the (3.6), while the second one recognizes the engine type and reads the thrust value from the related external database.

```

1  // Drag Thrust Intersection
2  double[] speed = MyArrayUtils.linspace(
3      SpeedCalc.calculateTAS(
4          0.05,
5          theCondition.get_altitude().getEstimatedValue()
6      ), // start
7      SpeedCalc.calculateTAS(
8          1.0,
9          theCondition.get_altitude().getEstimatedValue()
10     ), // ending
11     250 // points
12 );
13
14 List<DragMap> listDrag = new ArrayList<DragMap>();
15 for(int i=0; i<maxTakeOffMassArray.length; i++)
16     listDrag.add(
17         new DragMap(
18             weight[i],
19             theCondition.get_altitude().getEstimatedValue(),
20             DragCalc.calculateDragVsSpeed(
21                 weight[i],
22                 theCondition.get_altitude().getEstimatedValue(),
23                 aircraft.get_wing().get_surface().getEstimatedValue(),
24                 aircraft.get_theAerodynamics().get_cD0(),
25                 aircraft.get_wing().get_aspectRatio(),
26                 aircraft.get_theAerodynamics().get_owald(),
27                 speed,
28                 aircraft.get_wing().get_sweepHalfChordEq().getEstimatedValue(),
29                 aircraft.get_wing().get_maxThicknessMean(),
30                 AirfoilTypeEnum.MODERN_SUPERCRITICAL
31             ),
32             speed
33         )
34     );
35
36 List<ThrustMap> listThrust = new ArrayList<ThrustMap>();
37 for(int i=0; i<maxTakeOffMassArray.length; i++)
38     listThrust.add(
39         new ThrustMap(
40             theCondition.get_altitude().getEstimatedValue(),
41             1.0, // phi
42             ThrustCalc.calculateThrustVsSpeed(
43                 aircraft.get_powerPlant()
44                     .get_engineList().get(0).get_t0().getEstimatedValue(),
45                 1.0, // phi
46                 theCondition.get_altitude().getEstimatedValue(),
47                 EngineOperatingConditionEnum.CRUISE,
48                 EngineTypeEnum.TURBOFAN,
49                 aircraft.get_powerPlant().get_engineList().get(0).get_bpr(),
50                 aircraft.get_powerPlant().get_engineNumber(),
51                 speed
52             ),

```

```

53         speed,
54         aircraft.get_powerPlant().get_engineList().get(0).get_bpr(),
55         EngineOperatingConditionEnum.CRUISE
56     )
57 );
58
59 List<DragThrustIntersectionMap> intersectionList = PerformanceCalcUtils
60     .calculateDragThrustIntersection(
61         new double[] {theCondition.get_altitude().getEstimatedValue()},
62         speed,
63         weight,
64         new double[] {1.0},
65         new EngineOperatingConditionEnum[]
66             {EngineOperatingConditionEnum.CRUISE},
67         aircraft.get_powerPlant().get_engineList().get(0).get_bpr(),
68         aircraft.get_wing().get_surface().getEstimatedValue(),
69         cLmax,
70         listDrag,
71         listThrust
72     );
73 // Definition of a Mach array for each maxTakeOffMass
74 List<Double[]> machList = new ArrayList<Double[]>();
75 for(int i=0; i<maxTakeOffMassArray.length; i++)
76     machList.add(MyArrayUtils.linspaceDouble(
77         intersectionList.get(i).getMinMach(), // start
78         intersectionList.get(i).getMaxMach(), // ending
79         250)); // points

```

Listing 3.2 Intersection of drag and thrust curves in Specific Range test - B747-100B

At this point all static methods of the `SpecificRangeCalc` class are called in order to follow the flowchart steps of figure 3.7 with the purpose of calculating and plotting the cruise grid points.

```

1 // Calculation of the SFC for each Mach array
2 List<Double[]> sfcList = new ArrayList<Double[]>();
3 for(int i=0; i<maxTakeOffMassArray.length; i++)
4     sfcList.add(SpecificRangeCalc.calculateSfcVsMach(
5         machList.get(i),
6         theCondition.get_altitude().getEstimatedValue(),
7         aircraft.get_powerPlant().get_engineList().get(0).get_bpr(),
8         EngineTypeEnum.TURBOFAN
9     ));
10 // Calculation of the Efficiency for each Mach array
11 List<Double[]> efficiencyList = new ArrayList<Double[]>();
12 for(int i=0; i<maxTakeOffMassArray.length; i++)
13     efficiencyList.add(SpecificRangeCalc.calculateEfficiencyVsMach(
14         Amount.valueOf(maxTakeOffMassArray[i],SI.KILOGRAM),
15         machList.get(i),
16         aircraft.get_wing().get_surface().getEstimatedValue(),
17         theCondition.get_altitude().getEstimatedValue(),
18         aircraft.get_wing().get_aspectRatio(),
19         aircraft.get_theAerodynamics().get_oswald(),

```

```

20     aircraft.get_theAerodynamics().get_cD0(),
21     aircraft.get_wing().get_maxThicknessMean(),
22     aircraft.get_wing().get_sweepHalfChordEq(),
23     AirfoilTypeEnum.MODERN_SUPERCRITICAL));
24 // Calculation of the Specific range:
25 List<Double[]> specificRange = new ArrayList<Double[]>();
26 for (int i=0; i<maxTakeOffMassArray.length; i++)
27     specificRange.add(SpecificRangeCalc.calculateSpecificRangeVsMach(
28         Amount.valueOf(maxTakeOffMassArray[i], SI.KILOGRAM),
29         machList.get(i),
30         sfcList.get(i),
31         efficiencyList.get(i),
32         theCondition.get_altitude().getEstimatedValue(),
33         aircraft.get_powerPlant().get_engineList().get(0).get_bpr(),
34         0.85,
35         EngineTypeEnum.TURBOFAN));
36
37 // PLOTTING:
38 // building legend
39 List<String> legend = new ArrayList<String>();
40 for(int i=0; i<maxTakeOffMassArray.length; i++)
41     legend.add("MTOM = " + maxTakeOffMassArray[i] + " kg ");
42
43 SpecificRangeCalc.createSpecificRangeChart(specificRange, machList, legend);
44 SpecificRangeCalc.createSfcChart(sfcList, machList, legend,
45     EngineTypeEnum.TURBOFAN);
46 SpecificRangeCalc.createEfficiencyChart(efficiencyList, machList, legend);
47 SpecificRangeCalc.createThrustDragIntersectionChart(
48     theCondition.get_altitude().getEstimatedValue(),
49     maxTakeOffMassArray,
50     listDrag,
51     listThrust,
52     speed
53 );
54 // END OF THE TEST

```

Listing 3.3 Intersection of drag and thrust curves in Specific Range test - B747-100B

In conclusion, the following images shows the cruise grid, and all the evaluated quantities, calculated with this class and referred to the ATR-72 and of the B747-100B.

It's has to be noted that, as explained in the first paragraph, the maximum range condition is actually related to a low speed and also that, with a penalty of -1% in range, the specific range is about the same with a significantly higher speed; for example, in figure 3.15, the cruising Mach number, related to the maximum range condition of the B747-100B, varies, with the aircraft weight, between 0.74 and 0.80 while the long range one varies between 0.80 and 0.82, being more similar to the real cruising Mach number.

Moreover, the specific fuel consumption, from figures 3.10 and 3.11, grows with the Mach number, as expected, due to the major thrust given by engines; while the efficiency, from figures 3.12 and 3.13, decreases rapidly in the B747-100B case due to the increasing wave drag, not present in the ATR-72 case.

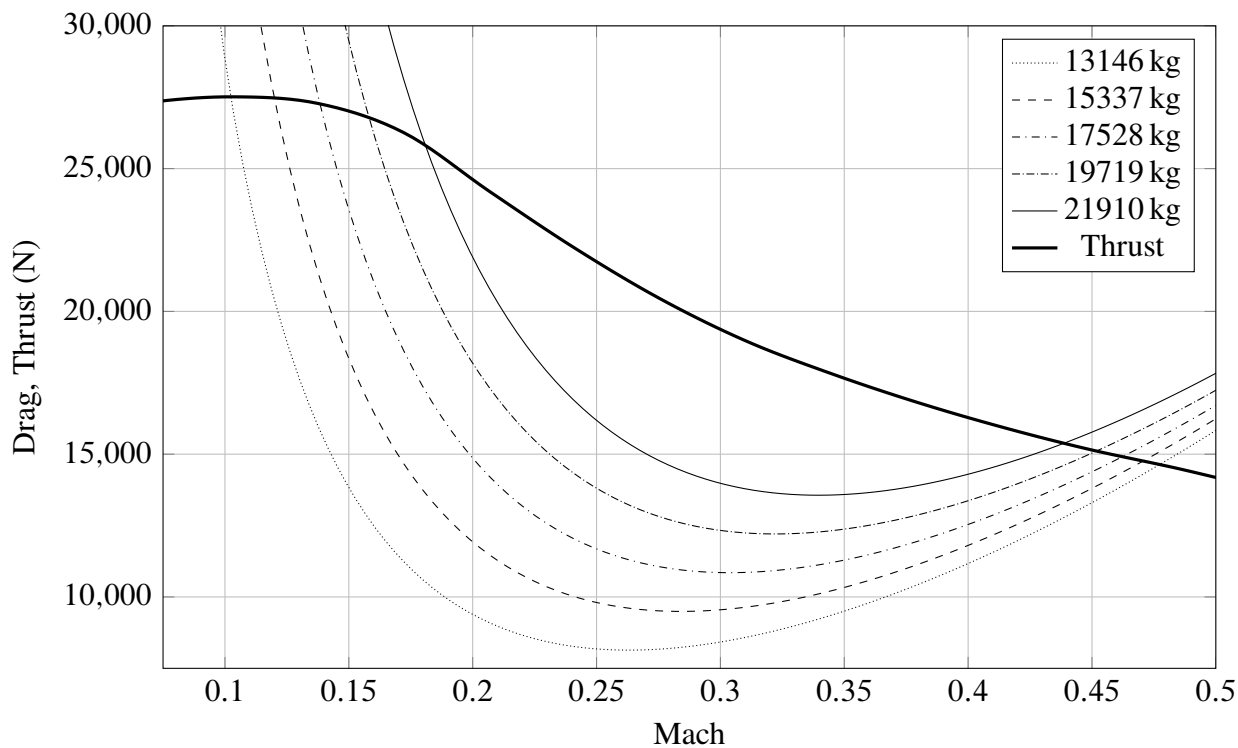


Figure 3.8 Intersection of drag and thrust curves at 6000m - ATR-72

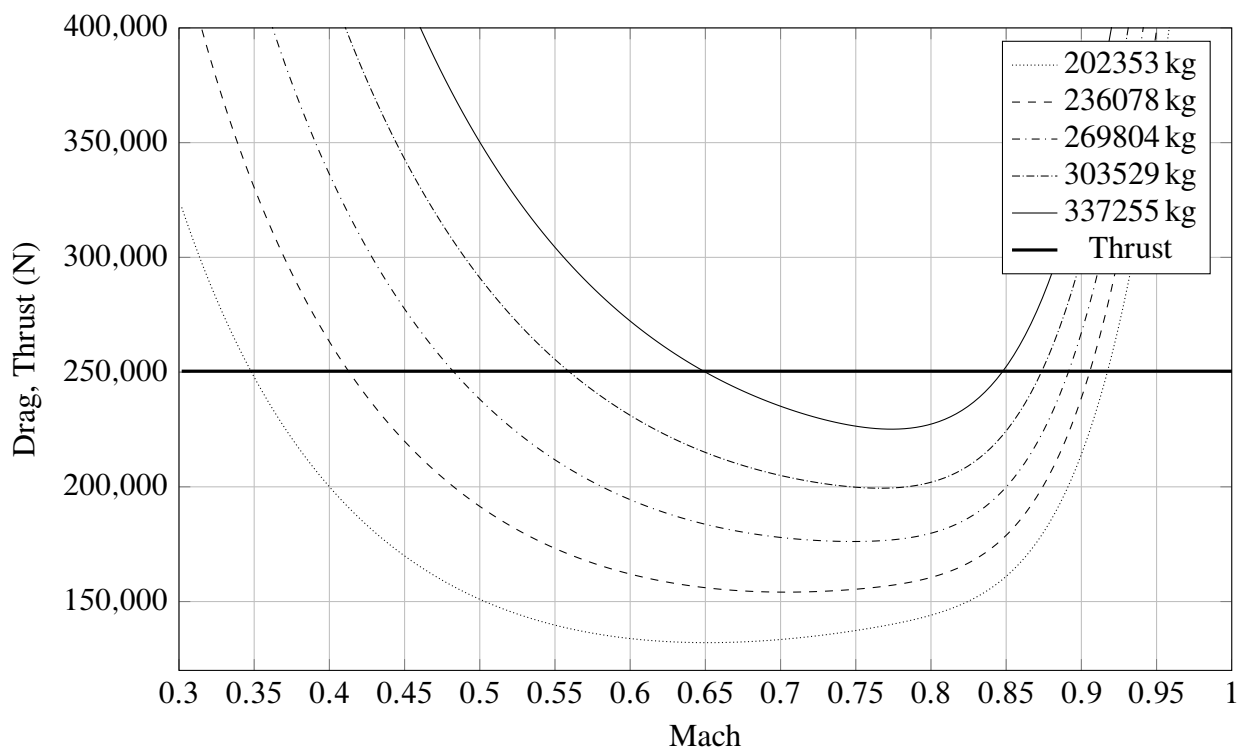


Figure 3.9 Intersection of drag and thrust curves at 10000m - B747-100B

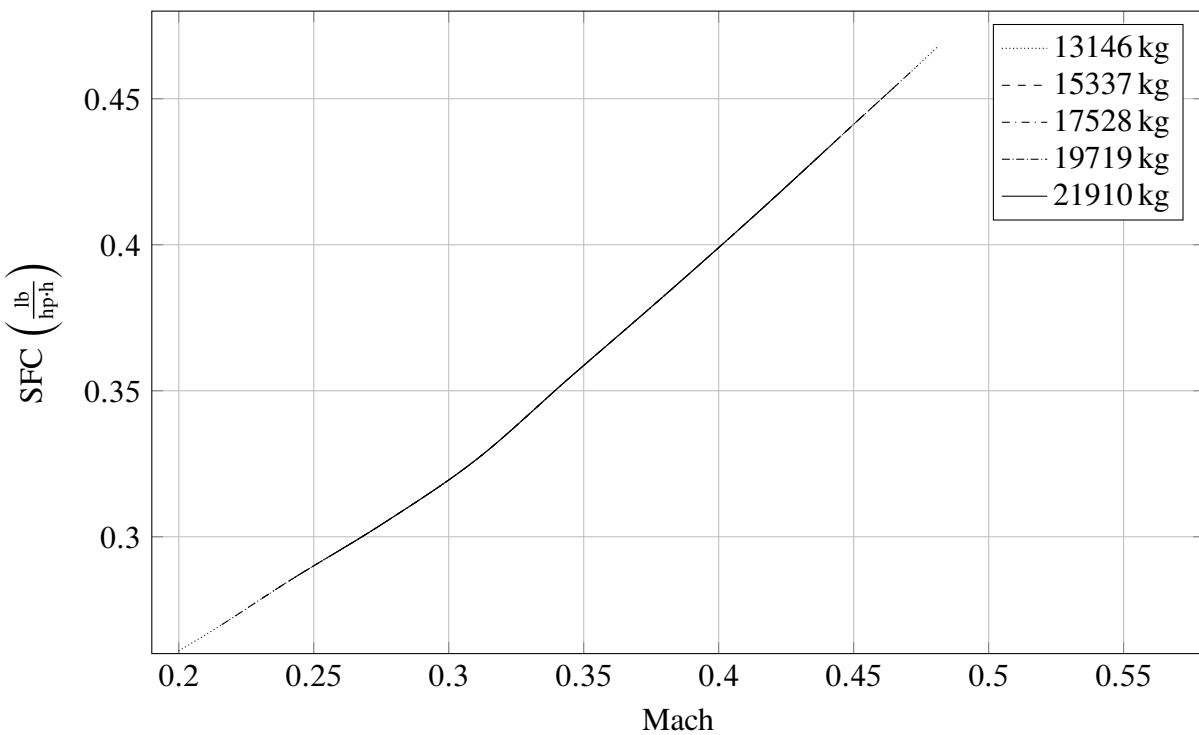


Figure 3.10 ATR-72 specific fuel consumption against Mach number at 6000m

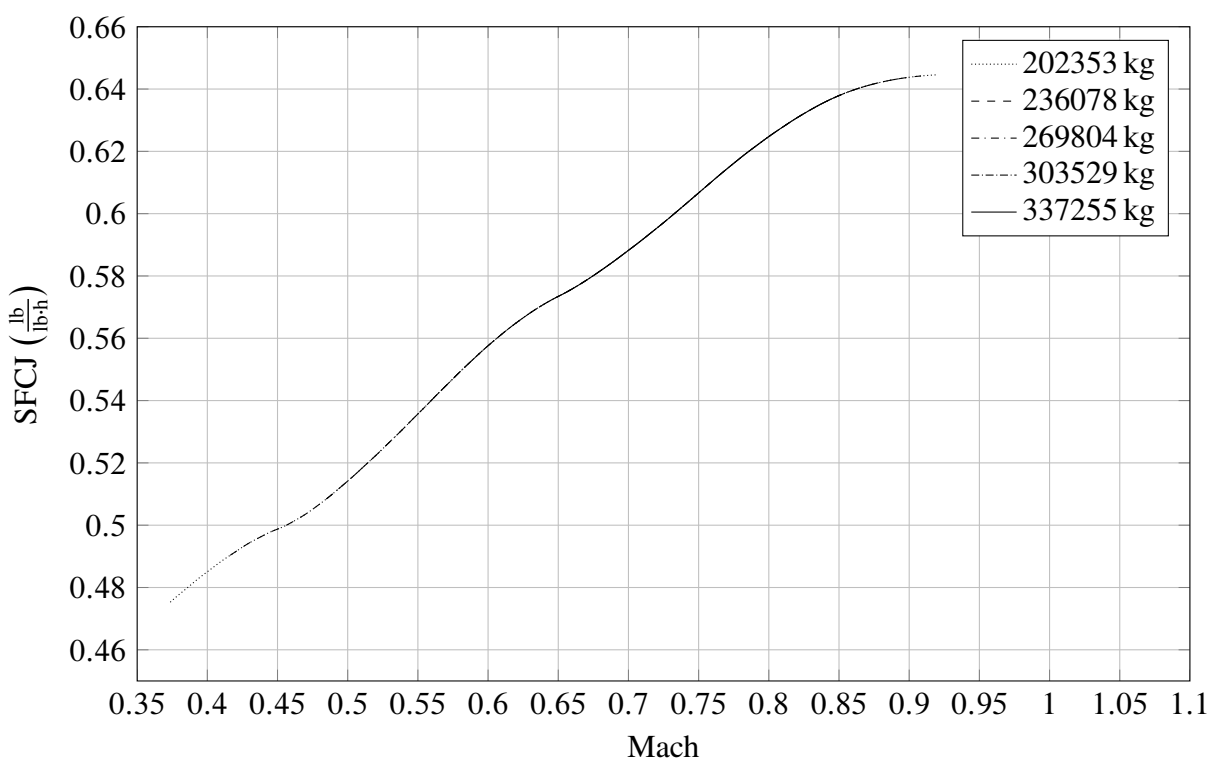


Figure 3.11 B747-100B specific fuel consumption against Mach number at 10000m

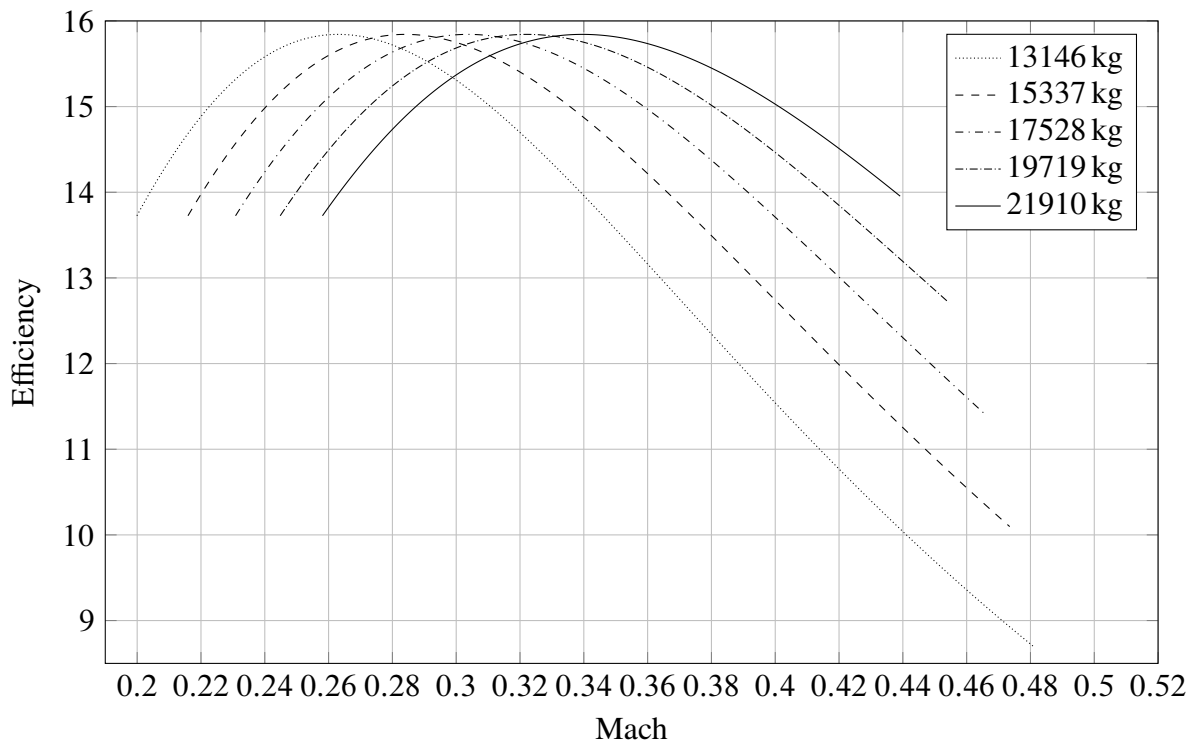


Figure 3.12 ATR-72 efficiency against Mach number at 6000m

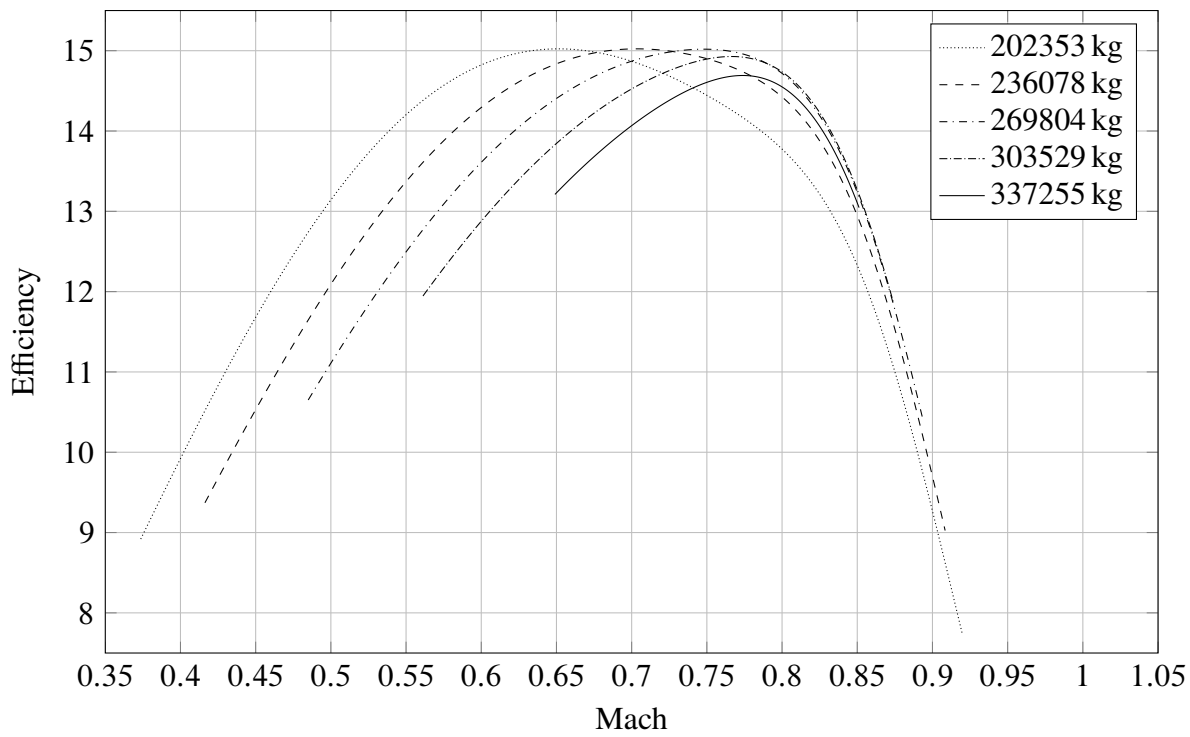
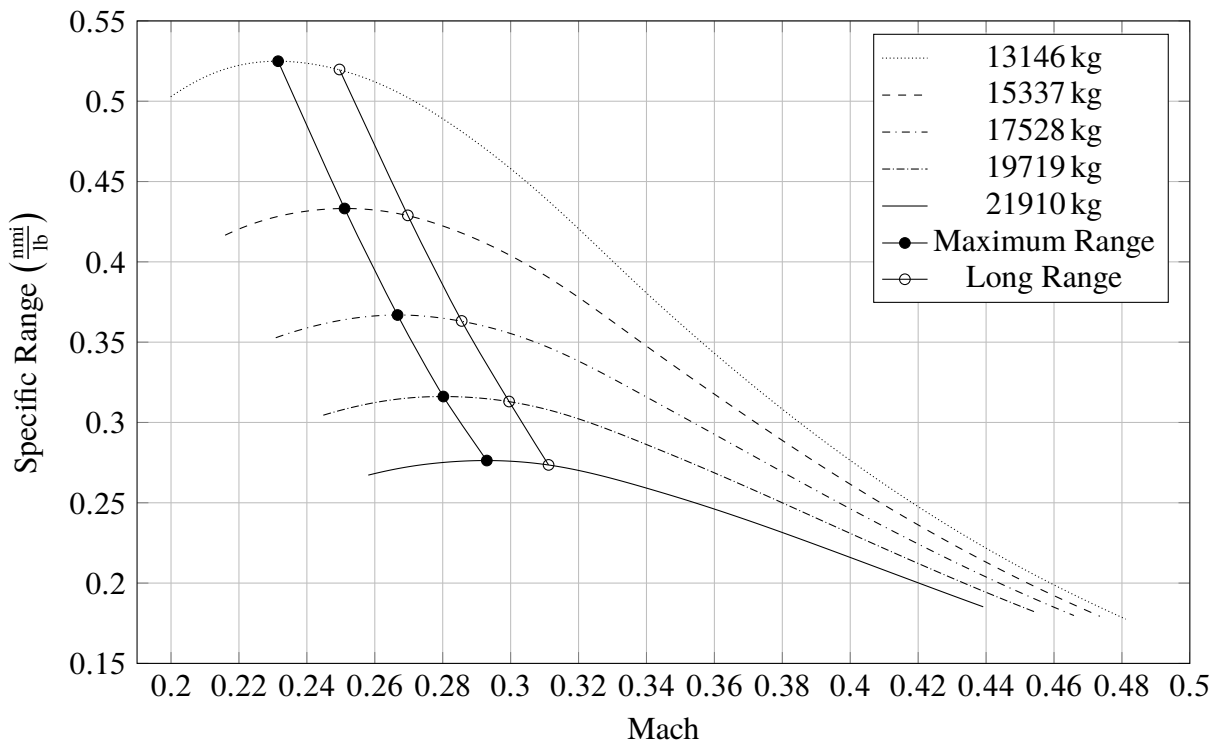
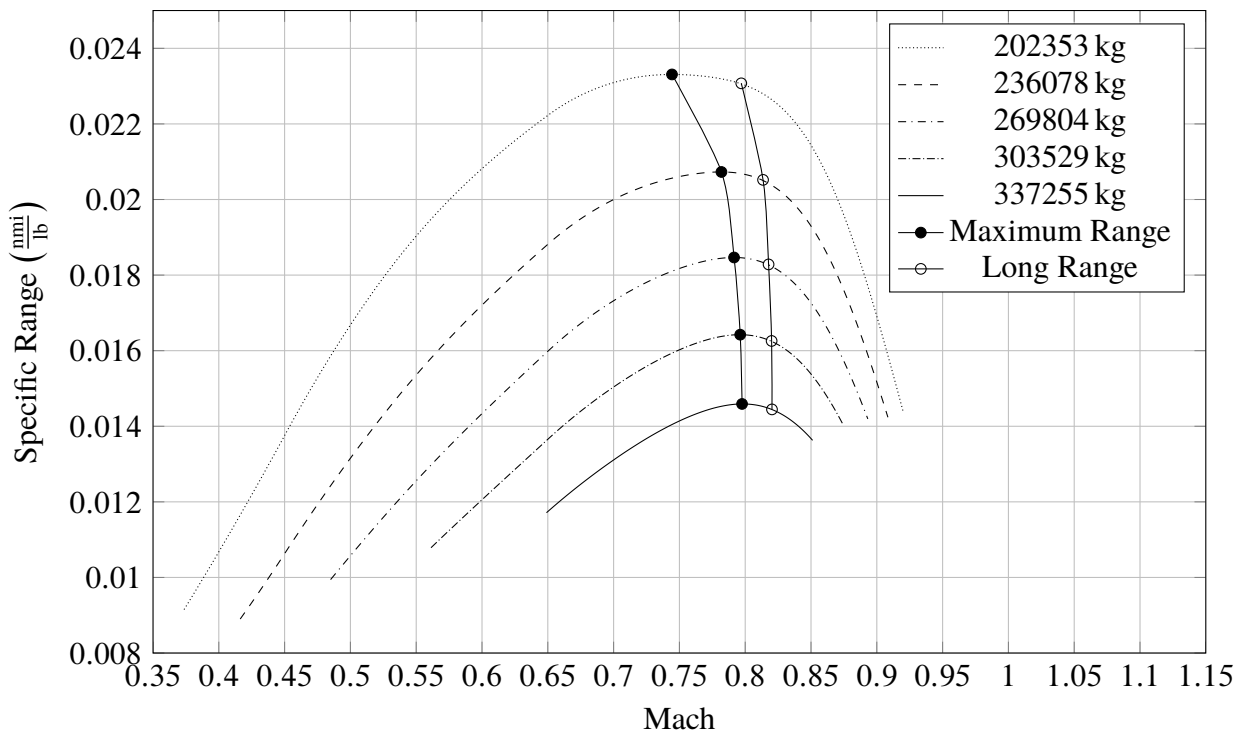


Figure 3.13 B747-100B efficiency against Mach number at 10000m

**Figure 3.14** ATR-72 cruise grid chart at 6000m**Figure 3.15** B747-100B cruise grid chart at 10000m

Chapter 4

HIGH LIFT DEVICES EFFECTS

In the preliminary design of the wing a large number of requirements have to be fulfilled as exemplified in table 4.1; but, as many of them are in conflict, it is hardly ever possible to check them all, so that a compromise has to be found.

Wing design requirements

- Low drag
 - High lift
 - Satisfactory maximum lift coefficient
 - Satisfactory stall quality
 - High value of the critical Mach number
 - Low weight
 - Ensure satisfactory performance in all flight phases
-

Table 4.1 Some wing design requirements

With respect of the last shown requirement, the wing is usually equipped with high-lift devices, which change its shape, in order to make it performant both in cruise both in take-off and landing phases. In fact, as can be seen from table 4.2, these phases show conflicting objectives which can only be mediated through the introduction of these devices.

Cruise requirements

- Small wing surface and high wing loading W/S
 - Small camber
 - Low drag
 - High speed
 - Lift generated using low c_L
-

Take-Off and Landing requirements

- Big wing surface, or high c_{Lmax} , in order to have an high equivalent wing loading $m = W/(S \cdot c_{Lmax})$
 - High drag value in landing
 - Lift generated using high c_L due to the low speed
-

Table 4.2 Comparison between cruise and take-off/landing design requirements

4.1 Theoretical background

In this paragraph, a general overview of the different type of high-lift devices is provided as well as the semi-empirical steps used to predict their effects on aerodynamic performance of the wing.

The designer may choose from a large collection of feasible high-lift systems, although in the case of a specific project this freedom will be limited, since incremental drag, mechanical complexity, development and maintenance costs and structural weight are all factors to be considered [30].

All high-lift devices can be divided in two main groups of which only the first one will be analyzed in this discussion:

- Systems for passive lift increase, such as *leading-edge devices* or *trailing-edge devices*, which modify the wing shape.
- Systems for active lift increase, such as *blown flaps* or *jet flaps*, which acts directly on the flow in order to control it.

Generally speaking, *trailing-edge devices* are used to increase the wing maximum lift coefficient, while *leading-edge devices* are used to increase the stalling angle of attack.

A more in depth analysis shows that *trailing-edge devices* increase the camber and improve the flow at the trailing edge, but tend to promote leading edge stall on thin sections and may cause a reduction in the stalling angle of attack; on the other hand *leading-edge devices* postpone or eliminate leading edge stall, but they have little effects on the airfoil camber as a whole, although locally the camber is increased [30].

About *trailing-edge devices*, their effects can be resumed in:

- Higher C_L at a given angle of attack and higher $C_{L_{\max}}$
- Lower stalling angle of attack
- Lower zero-lift angle due to increasing camber

while *leading-edge devices* provide the followings:

- Extension of the linear trait of the lift curve with an increase of the maximum angle of attack and of the $C_{L_{\max}}$
- Higher zero-lift angle due to translation of the lift curve on the right caused by leading edge deflection which reduce the actual angle of attack
- Higher slope of the linear trait of the lift curve, for those devices which extend airfoils chords with the effect of increase the wing surface and, with constant wing span, the aspect ratio

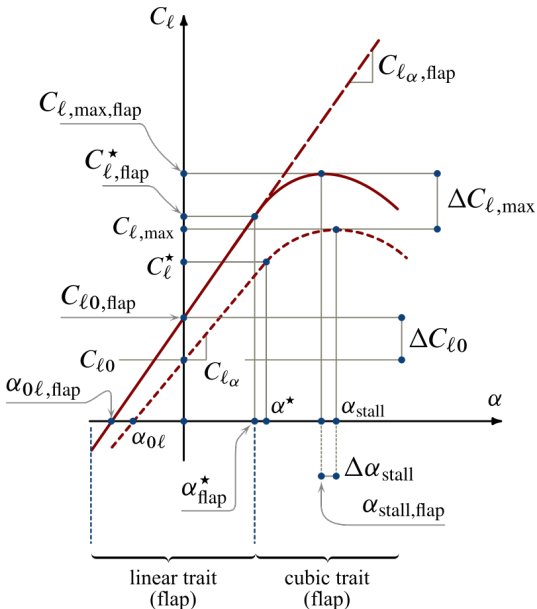


Figure 4.1 Trailing-edge devices effects

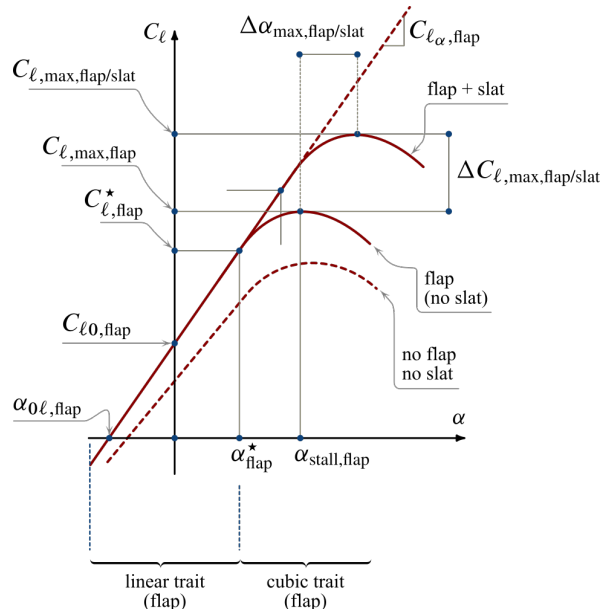


Figure 4.2 Leading-edge devices effects

Among the variety of different devices, only the followings will be taken into account as they represents the most used ones.

Plain flap This device is most used on small aircraft or ones equipped of a thin wing because it doesn't support a complex mechanism of retraction. Typical deflections are about 20° for take-off and 60° for landing.

Single slotted flap It can be seen as a plain flap with a gap between the two elements composing the airfoil. The single slotted flap has very little flap overlap with the fixed trailing edge and hence develops only little Fowler motion, that is the aft travel of the flap that increases the section chord. Its typical deflections are about 20° for take-off and 40° for landing.

The effects of a single slotted flap show an increment in all the aerodynamic coefficients, but it must be said that the increment in drag is lower than that for plain flaps. The slotted flap chord usually ranges from the 25% up to the 30% of the section chord. Moreover the slot influences boundary layer control, in fact it introduces a blowing that energizes the boundary layer delaying separation, so an increase in lift is generated.

Double slotted flap This device is superior to the previous type at large deflections, because separation of the flow over the flap is postponed by the more favourable pressure distribution. Its typical deflections are about 20° for take-off and 50° for landing; in particular, in order to avoid an increasing twisting moment due the deflection, this devices are usually combined with leading edge slats deflected of the same quantity.

Triple slotted flap This device is used on several transport aircraft with very high wing loadings. In combination with leading edge devices, this system represents almost the ultimate achievement in passive high-lift technology, but its shape shows that complicated flap supports and controls are required. Its typical deflections are about 20° for take-off and 40° for landing.

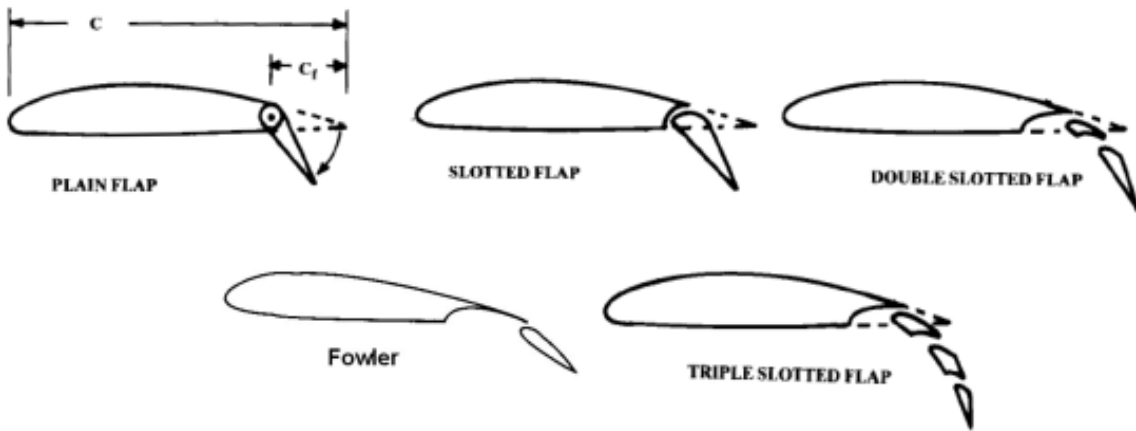


Figure 4.3 Analyzed trailing edge devices types

Fowler flap It is theoretically a single slotted flap that adds to the downward deflection also a backward motion that allows the increment of the effective chord and camber.

Due to the necessity of keeping the rear part of the wing section extended out the main element its implementation system is usually more complicated than the single slotted flaps but its weight and costs are largely justified by its high lift effectiveness. Its typical deflection are about 40° for landing and 15° for take-off, smaller than other types because the chord extension provides a bigger lift increment due to the bigger wing surface; this also reduces the drag in take-off wth benefit an the required field length.

Slat It's the most efficient leading edge device; thanks to combined deflection and forward motion, it acts in order to increase airfoil camber, and so the maximum lift coefficient, as well as increase the airfoil chord with the result of a bigger surface which provides a bigger aspect ratio with the effect of increase the lift curve slope of the linear trait. Furthermore, thanks to the slot which provides a boundary layer energization, it also increases the stalling angle of attack.

Kruger flap It acts in the same way as the slat, but it is thinner and more suitable for installation on thin wings. Krueger flaps are very common because of their simple architecture.

Plain leading edge flap Is less effective than slat since it has no slot, it is mechanically simple and rigid and particularly suitable for thin airfoil sections. The leading edge can be hinged in order to move it backward (droop nose) or it has a mechanism inside that changes the curvature of the nose (variable camber flap).

Leading edge fixed slot It has a fixed slot at the leading edge that, at high angle of attack, allows the airflow to pass through energizing the boundary layer; this helps to increase the stalling angle of attack. During the criuse phase, in which the angle of attack is small, the gap is usually sealed.

In order to predict, from the preliminary design phase, the aerodynamic characteristics of the high-lift devices, some useful semi-empirical methods are available; in this particular case the followings formulas and charts are taken from [30] and [26].

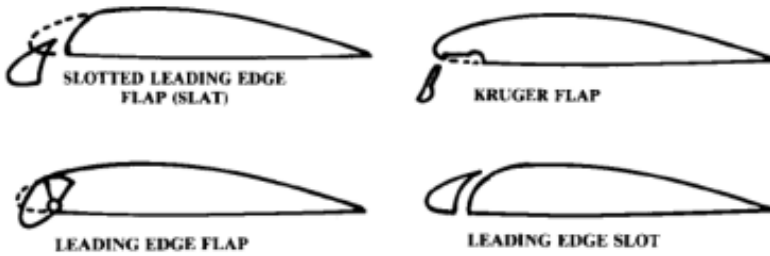


Figure 4.4 Analyzed leading edge devices types

The guideline that will be followed provides to analyze separately the trailing edge and the leading edge devices effects; moreover it will start by evaluating the changes in aerodynamic characteristics of airfoils for then extends these to entire wing.

From figures 4.1 and 4.2, it's possible to understand that the main changes introduced by trailing edge, or leading edge, devices are related to the evaluation of four quantities:

- ΔC_{l0}
- $\Delta C_{l\max}$
- $C_{l\alpha,\text{flap}}$
- $\Delta\alpha_{\text{stall}}$

4.1.1 ΔC_{l0} and ΔC_{L0} calculation

An empirical method for predicting airfoil lift increments at zero angle of attack for high-lift systems (Δc_{l0}) comes from the Glauert's linearized theory for thin airfoils with flaps. A result obtained from this theory for the lift due to flap deflection is the following.

$$\alpha_\delta = 1 - \frac{\theta_f - \sin(\theta_f)}{\pi} \quad (4.1)$$

where

$$\theta_f = \cos^{-1} \left(2 \frac{c_f}{c} - 1 \right) \quad (4.2)$$

Known this value, it's possible to evaluate the theoretical Δc_{l0} which can be calculated as proposed in (4.3).

$$\Delta C_{l0} = \alpha_\delta C_{l\alpha} \delta_f \quad (4.3)$$

with $C_{l\alpha}$ equals to the linear slope of the lift curve of the airfoil, and δ_f the flap angular deflection.

For large flap deflections and for the separation at large flap angles due to viscosity, linear theory is in error when compared with exact one, for this reason we assume the effectiveness factor η_δ , so the formulation becomes the following.

$$\Delta C_{l0} = \alpha_\delta C_{l\alpha} \delta_f \eta_\delta \quad (4.4)$$

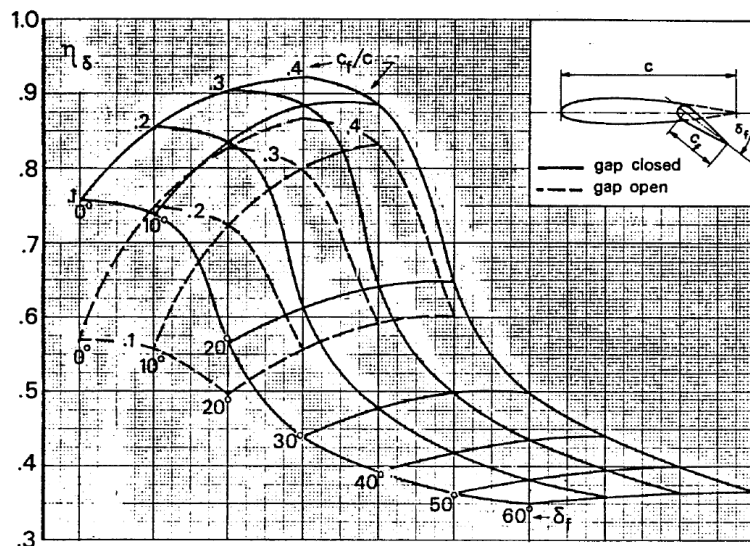


Figure 4.5 η_δ for plain flap

where η_δ can be evaluated from the charts provided in figures 4.5 and 4.6.

In case of flaps which extend the airfoil chord, this effect also contributes to the lift increase and can be taken into account by referring the section lift to the extended chord and then converting the result to the original chord. As a result of this, the section lift coefficient can be evaluated as shown in (4.5).

$$C_l = (C'_{l0} + \Delta C'_{l0}) \frac{c'}{c} \quad (4.5)$$

where the variables with superscript are referred to the extended chord. Assuming that for the basic section $c'_{l0} = c_{l0}$, it's possible to derive the Δc_{l0} as follows.

$$\Delta C_{l0} = \Delta C'_{l0} \frac{c'}{c} + C_{l0} \left(\frac{c'}{c} - 1 \right) \quad (4.6)$$

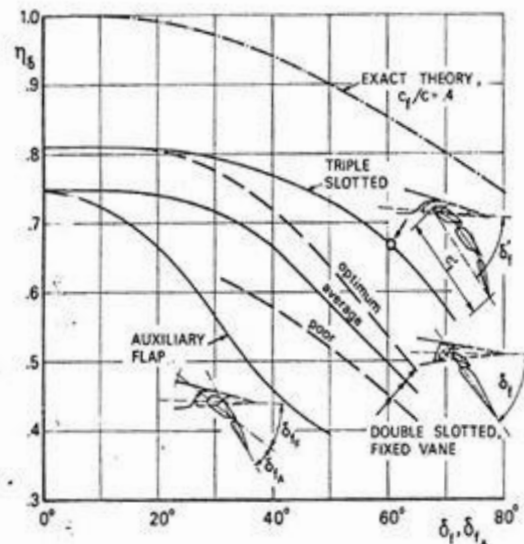
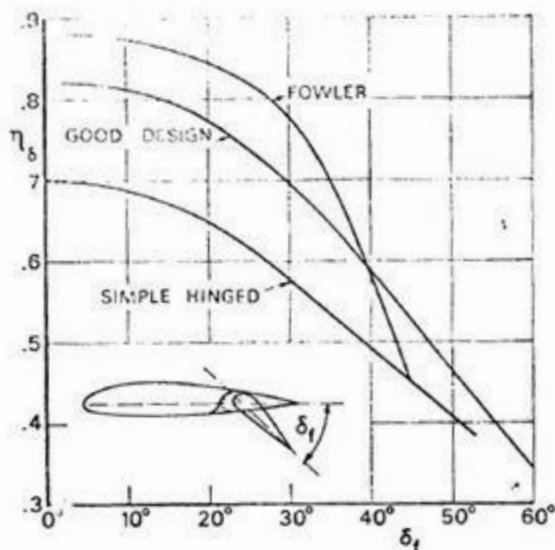


Figure 4.6 η_δ for other type of flaps

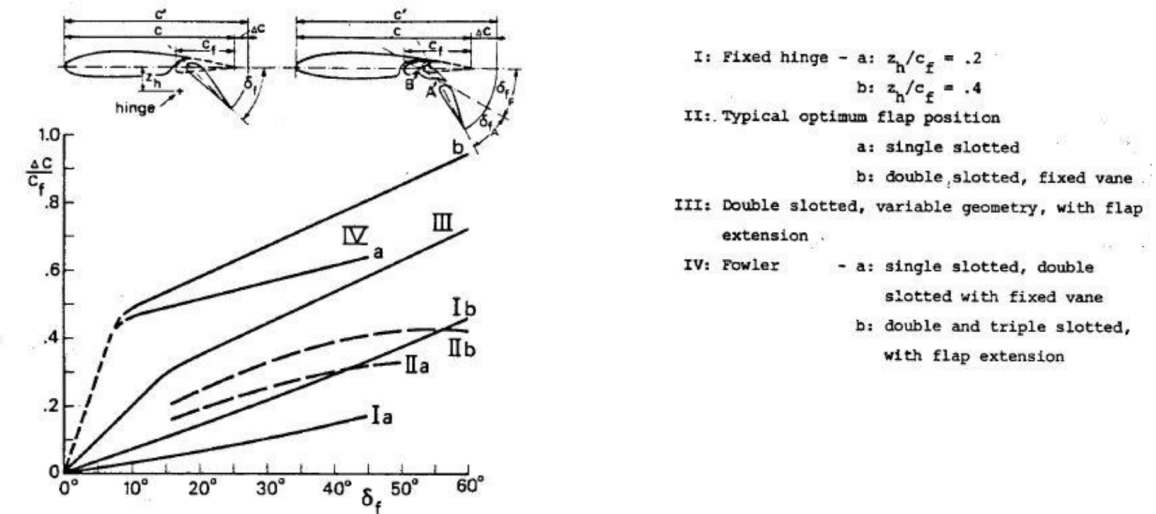


Figure 4.7 $\frac{\Delta c}{c_f}$ for different type of flaps as function of flap deflection

in which C_{l0} is known, $\Delta C'_{l0}$ is calculated as in (4.4) and $\frac{c'}{c}$ is equal to the following expression.

$$\frac{c'}{c} = 1 + \frac{\Delta c}{c_f} \frac{c_f}{c} \quad (4.7)$$

where $\frac{\Delta c}{c_f}$ can be derived from the charts of figure 4.7.

The ΔC_{l0} so calculated has now to be extended to the entire wing; this can be through the following formula.

$$\Delta C_{L0} = \Delta C_{l0} \left(\frac{C_{L\alpha}}{C_{l\alpha}} \right) \left[\frac{(\alpha_\delta)_{C_L}}{(\alpha_\delta)_{C_l}} \right] K_b \quad (4.8)$$

where $C_{L\alpha}$ and $C_{l\alpha}$ are respectively the lift curve slopes of the wing and the airfoil, $\left[\frac{(\alpha_\delta)_{C_L}}{(\alpha_\delta)_{C_l}} \right] = K_c$ is the ratio of the three-dimensional flap effectiveness parameter to the two dimensional flap effectiveness one, which can be derived from the figure 4.8, and K_b is a flap span effectiveness factor, which is function of the flap span-wise extension, that can be read from 4.9.

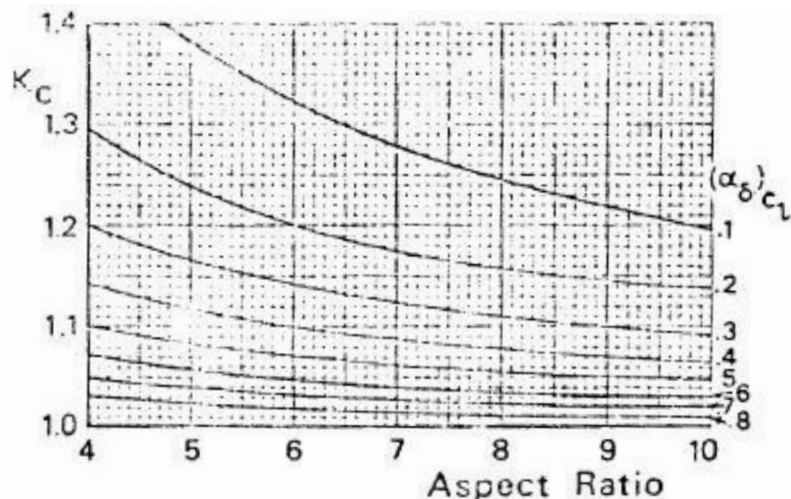


Figure 4.8 K_c for different $(\alpha_\delta)_{C_L}$ as function of wing aspect ratio

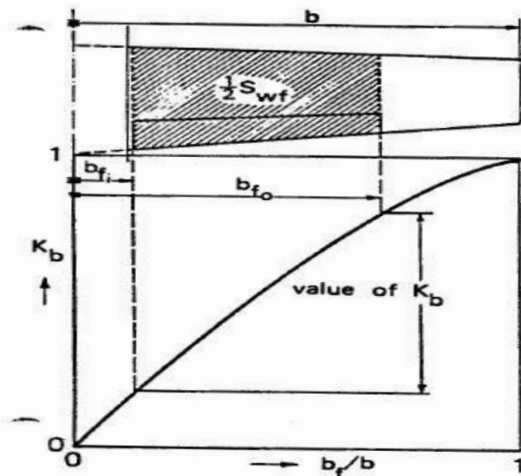


Figure 4.9 K_b as function of flap span to wing span ratio ($\frac{b_f}{b}$)

4.1.2 $\Delta C_{l\max}$ and $\Delta C_{L\max}$ calculation for flaps and slats

4.1.3 $C_{l\alpha,\text{flap}}$ and $C_{L\alpha,\text{flap}}$ calculation

4.1.4 $\Delta\alpha_{\text{stall}}$ calculation for flaps and slats

4.1.5 Further effects calculations

4.2 Java class architecture

4.3 Case study: ATR-72 and B747-100B

Chapter **5**

TAKE-OFF PERFORMANCE

5.1 Theoretical background

5.2 Java class architecture

5.3 Case study: B747-100B

Appendices

Appendix

A

HDF DATABASE CREATION AND READING

A.1 Creation of a database using MATLAB

Creation and mangment of an HDF Dataset are very important to handle because they allow to generate resources which are required by a lot of analysis; for example by using this datasets it's possible to implement a new engine type allowing the analysis of the preformance of a new aircraft. This feature has not been implemented inside JPAD with the purpose of being able to generate the required resources independently.

First of all it's necessary to have curves of the database that has to be digitalized; then, with the use of sotware like *PlotDigitizer*, it's possible to acquire them using a finite number of points chosen by the user. The output of this procedure is a *.csv* file containing all the copule of points which have been used to digitalize the specific curve.

Now the matlab code comes in play to manage these data and to generate the digitalized curves and the HDF dataset. In the example reported there are four curves defined by points through *PlotDigitizer* which have, firstly, been imported in MATLAB generating four *.mat* files; at this point the code interpolates curves points with cubic splines in order to have more points to plot for each curve.

Finally curves are plotted and the HDF Dataset is populated by using *h5create* and *h5write*; in particular curves points, abscissas and parameterization values are attached to the h5 file through these commands.

Listing A.1 MATLAB script for creating the HDF Database

```
1 clc; close all; clear all;
2
3 %% Import data
4 DeltaAlphaCLmax_vs_LambdaLE_dy1p2 =
    importdata('DeltaAlphaCLmax_vs_LambdaLE_dy1p2.mat');
5 DeltaAlphaCLmax_vs_LambdaLE_dy2p0 =
    importdata('DeltaAlphaCLmax_vs_LambdaLE_dy2p0.mat');
```

```

6 DeltaAlphaCLmax_vs_LambdaLE_dy3p0 =
    importdata('DeltaAlphaCLmax_vs_LambdaLE_dy3p0.mat');
7 DeltaAlphaCLmax_vs_LambdaLE_dy4p0 =
    importdata('DeltaAlphaCLmax_vs_LambdaLE_dy4p0.mat');
8
9 nPoints = 30;
10 lambdaLEVector_deg = transpose(linspace(0, 40, nPoints));
11
12 %% dy/c = 1.2
13 smoothingParameter = 0.999999;
14 DAlphaVsLambdaLESplineStatic_Dy1p2 = csaps( ...
15     DeltaAlphaCLmax_vs_LambdaLE_dy1p2(:,1), ...
16     DeltaAlphaCLmax_vs_LambdaLE_dy1p2(:,2), ...
17     smoothingParameter);
18 DAlphaVsLambdaLEStatic_Dy1p2 = ppval( ...
19     DAlphaVsLambdaLESplineStatic_Dy1p2, ...
20     lambdaLEVector_deg);
21
22 %% dy/c = 2.0
23 smoothingParameter = 0.999999;
24 DAlphaVsLambdaLESplineStatic_Dy2p0 = csaps( ...
25     DeltaAlphaCLmax_vs_LambdaLE_dy2p0(:,1), ...
26     DeltaAlphaCLmax_vs_LambdaLE_dy2p0(:,2), ...
27     smoothingParameter);
28 DAlphaVsLambdaLEStatic_Dy2p0 = ppval( ...
29     DAlphaVsLambdaLESplineStatic_Dy2p0, ...
30     lambdaLEVector_deg);
31
32 %% dy/c = 3.0
33 smoothingParameter = 0.999999;
34 DAlphaVsLambdaLESplineStatic_Dy3p0 = csaps( ...
35     DeltaAlphaCLmax_vs_LambdaLE_dy3p0(:,1), ...
36     DeltaAlphaCLmax_vs_LambdaLE_dy3p0(:,2), ...
37     smoothingParameter);
38 DAlphaVsLambdaLEStatic_Dy3p0 = ppval( ...
39     DAlphaVsLambdaLESplineStatic_Dy3p0, ...
40     lambdaLEVector_deg);
41
42 %% dy/c = 4.0
43 smoothingParameter = 0.999999;
44 DAlphaVsLambdaLESplineStatic_Dy4p0 = csaps( ...
45     DeltaAlphaCLmax_vs_LambdaLE_dy4p0(:,1), ...
46     DeltaAlphaCLmax_vs_LambdaLE_dy4p0(:,2), ...
47     smoothingParameter);
48 DAlphaVsLambdaLEStatic_Dy4p0 = ppval( ...
49     DAlphaVsLambdaLESplineStatic_Dy4p0, ...
50     lambdaLEVector_deg);
51
52 %% Plots
53 figure(1)
54 plot(lambdaLEVector_deg, DAlphaVsLambdaLEStatic_Dy1p2, '-*b' ... , ... );
55 hold on;
56 plot(lambdaLEVector_deg, DAlphaVsLambdaLEStatic_Dy2p0, '-b' ... , ... );

```

```

57 plot (lambdaLEVector_deg, DALphaVsLambdaLEStatic_Dy3p0, '*b' ... , ...);
58 plot (lambdaLEVector_deg, DALphaVsLambdaLEStatic_Dy4p0, 'b' ... , ...);
59 xlabel ('\Lambda_{le} (deg)'); ylabel ('\Delta\alpha_{C_{L,max}}');
60 title ('Angle of attack increment for wing maximum lift in subsonic flight');
61 legend ('\Delta y/c = 1.2', '\Delta y/c = 2.0', '\Delta y/c = 3.0', '\Delta y/c =
        4.0');
62 axis ([0 50 0 9]);
63 grid on;
64
65 %% preparing output to HDF
66 % dy/c
67 dyVector = [1.2;2.0;3.0;4.0];
68 %columns --> curves
69 myData = [ ...
70     DALphaVsLambdaLEStatic_Dy1p2, ...
71     DALphaVsLambdaLEStatic_Dy2p0, ...
72     DALphaVsLambdaLEStatic_Dy3p0, ...
73     DALphaVsLambdaLEStatic_Dy4p0];
74
75 hdfFileName = 'DALphaVsLambdaLEVsDy.h5';
76 if ( exist(hdfFileName, 'file') )
77     fprintf('file %s exists, deleting and creating a new one\n', hdfFileName);
78     delete(hdfFileName)
79 else
80     fprintf('Creating new file %s\n', hdfFileName);
81 end
82 % Dataset: data
83 h5create(hdfFileName, '/DALphaVsLambdaLEVsDy/data', size(myData));
84 h5write(hdfFileName, '/DALphaVsLambdaLEVsDy/data', myData);
85 % Dataset: var_0
86 h5create(hdfFileName, '/DALphaVsLambdaLEVsDy/var_0', size(dyVector));
87 h5write(hdfFileName, '/DALphaVsLambdaLEVsDy/var_0', dyVector);
88 % Dataset: var_1
89 h5create(hdfFileName, '/DALphaVsLambdaLEVsDy/var_1', size(lambdaLEVector_deg));
90 h5write(hdfFileName, '/DALphaVsLambdaLEVsDy/var_1', lambdaLEVector_deg);

```

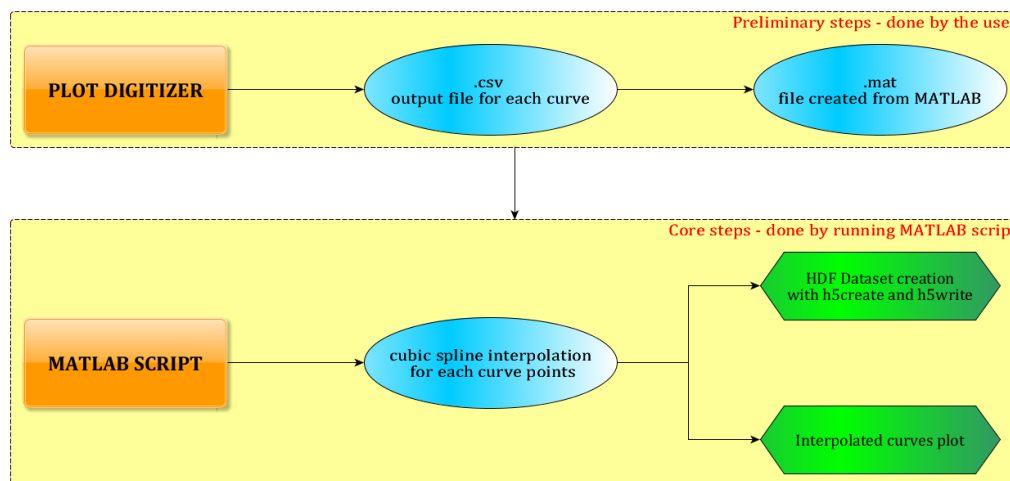


Figure A.1 Flowchart of an HDF Database creation

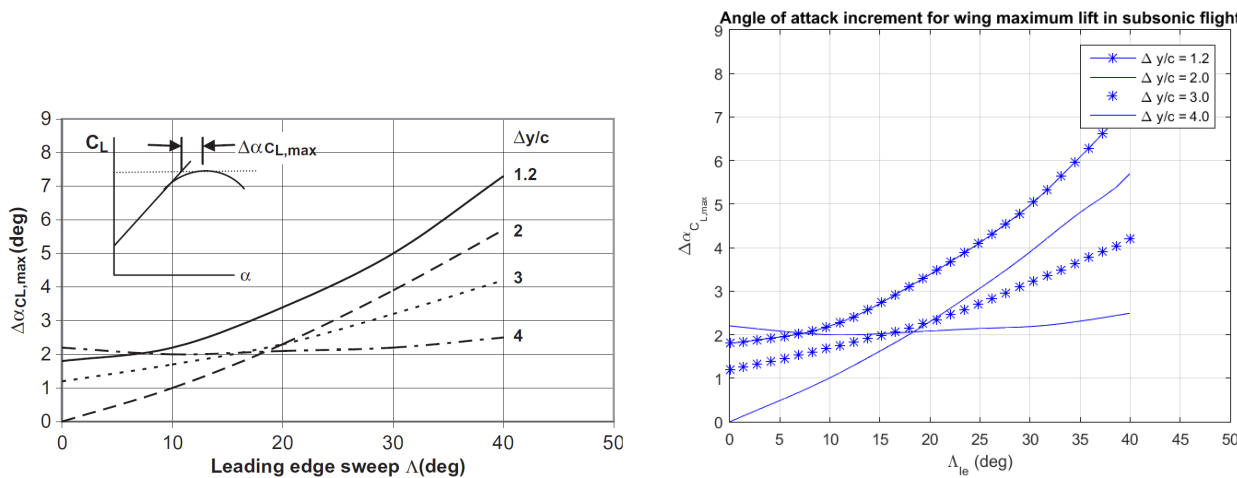


Figure A.2 Comparison between the initial graph and the digitized one

A.2 Reading data from an HDF database in JPAD

After creating the database, this has to be read in order to obtain the required data; inside JPAD this operation can be done defining a specific class, which extends the abstract class `DatabaseReader` that is designed for HDF dataset reading.

This son class has a specific structure which main key points can be summarized in the following ones:

1. Creation of variables, in number equal to the function to be interpolated, using the type `MyInterpolatingFunction`
2. Creation of variables for all values that are wanted to be read from the interpolating functions
3. Creation of a builder that accepts the folder path string and the file name string of the database. This builder has to launch the interpolating method for all functions contained into the database by using `MyInterpolatingFunction` methods.
4. Creation of a getter method for each of the variables allocated at point 2 in order to obtain values from interpolated functions by giving in input the required parameters

In particular the class `MyInterpolatingFunction` implements methods for a spline, bicubic and tricubic data interpolation as well as three methods for extracting a specific value from each of the previous interpolated curve.

The following listing describes, with an example upon the aerodynamic database, how the reader class should be build following the previous steps.

Listing A.2 DatabaseReader son class creation

```

1 public class AerodynamicDatabaseReader extends DatabaseReader {
2     // STEP 1:
3     private MyInterpolatingFunction
4         c_m0_b_k2_minus_k1_vs_FFR,
5         ar_v_eff_c2_vs_Z_h_over_b_v_x_ac_h_v_over_c_bar_v;

```

```
6 // STEP 2:  
7     double cM0_b_k2_minus_k1, ar_v_eff_c2;  
8 // STEP 3:  
9     public AerodynamicDatabaseReader(String databaseFolderPath, String  
10         databaseFileName) {  
11         super(databaseFolderPath, databaseFileName);  
12         c_m0_b_k2_minus_k1_vs_FFR =  
13             database.interpolate1DFromDatasetFunction(  
14                 "(C_m0_b)_k2_minus_k1_vs_FFR"  
15             );  
16         ar_v_eff_c2_vs_Z_h_over_b_v_x_ac_h_v_over_c_bar_v =  
17             database.interpolate2DFromDatasetFunction(  
18                 "(AR_v_eff)_c2_vs_Z_h_over_b_v_(x_ac_h--v_over_c_bar_v)"  
19             );  
20     }  
21 // STEP 4:  
22     public double get_C_m0_b_k2_minus_k1_vs_FFR(double length, double diameter) {  
23         return c_m0_b_k2_minus_k1_vs_FFR.value(length/diameter);  
24     }  
25 // STEP 4:  
26     public double get_AR_v_eff_c2_vs_Z_h_over_b_v_x_ac_h_v_over_c_bar_v(double zH,  
27         double bV, double xACHV, double cV) {  
28         return ar_v_eff_c2_vs_Z_h_over_b_v_x_ac_h_v_over_c_bar_v.value(zH/bV, xACHV/cV);  
29     }
```

BIBLIOGRAPHY

- [1] L. Attanasio. «Development of a Java Application for Parametric Aircraft Design». Master thesis. University of Naples "Federico II", 2014.
- [2] Various Authors. *ATR 72*. URL: https://en.wikipedia.org/wiki/ATR_72.
- [3] Various Authors. *Boeing 747*. URL: https://en.wikipedia.org/wiki/Boeing_747.
- [4] Various Authors. *eXtensible Markup Language (XML)*. URL: <https://en.wikipedia.org/wiki/XML>.
- [5] S. Ciornei. *Mach number, relative thickness, sweep and lift coefficient of the wing - An empirical investigation of parameters and equations*. Paper. 31.05.2005.
- [6] Oracle Corporation. *List*. URL: <https://docs.oracle.com/javase/8/docs/api/java/util/List.html>.
- [7] Jean-Marie Dautelle. *Jscience*. URL: <http://jscience.org/>.
- [8] E. De Bono. «Prestazioni di decollo e atterraggio. Calcolo approssimato e verifica sperimentale.» Thesis. University of Naples "Federico II", 2011.
- [9] D. et al Gilbert. *JFreeChart*. URL: <http://www.jfree.org/jfreechart/>.
- [10] The HDF Group. *HDF*. URL: <https://www.hdfgroup.org/products/java/hdf-javadoc/html/javadocs/ncsa/hdf/hdf5lib/H5.html>.
- [11] W.F. Hilton. *High-speed Aerodynamics*. Longmans, Green, 1951.
- [12] D. Howe. *Aircraft conceptual design synthesis*. Aerospace Series. Professional Engineering Publishing, 2000.
- [13] J. Huwaldt. *1976 Standard Atmosphere Program*. URL: <http://thehuwaldtfamily.org/java/Applications/StdAtmosphere/StdAtmosphere.html>.
- [14] P. Jackson and FRAeS. *Jane's All the World's Aircraft*. Jane's All the World's Aircraft. Jane's Information Group, 2004-2005.
- [15] L.R. Jenkinson, D. Rhodes, and P. Simpkin. *Civil jet aircraft design*. AIAA education series. Arnold, 1999.
- [16] K. Kawaguchi. *Args4j*. URL: <http://args4j.kohsuke.org/>.
- [17] I. Kroo and R. Shevell. *Aircraft Design: Synthesis and Analysis*. 1999.
- [18] A. Lausetti. *Decollo e atterramento di aeroplani, idrovolanti trasportati*. Levrotto & Bella Editrice S.a.s., 1992.

-
- [19] B. W. McCormick. *Aerodynamics, Aeronautics, and Flight Mechanics*. John Wiley & Sons, 1979.
 - [20] L.M. Nicolai and G. Carichner. *Fundamentals of Aircraft and Airship Design*. AIAA education series v. 1. American Institute of Aeronautics and Astronautics, 2010.
 - [21] F. Nicolosi and G. Paduano. *Behind ADAS*. 2011.
 - [22] E. Obert. *Aerodynamic Design of Transport Aircraft*. IOS Press, 2009.
 - [23] D.P. Raymer. *Aircraft Design: A Conceptual Approach*. 1992.
 - [24] D.P. Raymer. *Aircraft Design / RDS-Student: A Conceptual Approach*. AIAA Education Series. Amer Inst of Aeronautics &, 2013.
 - [25] M.H. Sadraey. *Aircraft Design: A Systems Engineering Approach*. Aerospace Series. Wiley, 2012.
 - [26] P.M. Sforza. *Commercial Airplane Design Principles*. Elsevier Science, 2014.
 - [27] E. Torenbeek. *Advanced Aircraft Design: Conceptual Design, Technology and Optimization of Subsonic Civil Airplanes*. Aerospace Series. Wiley, 2013.
 - [28] E. Torenbeek. *Optimum Cruise Performance of Subsonic Transport Aircraft*. Delft University Press, 1998.
 - [29] E. Torenbeek. *Synthesis of Subsonic Aircraft Design*. 1976.
 - [30] E. Torenbeek. *Synthesis of Subsonic Airplane Design: An Introduction to the Preliminary Design of Subsonic General Aviation and Transport Aircraft, with Emphasis on Layout, Aerodynamic Design, Propulsion and Performance*. Springer, 1982.
 - [31] A.D. Young. *The Aerodynamic Characteristics of Flaps*. Technical Report. 1947.

GLOSSARY

Autonomy Factor Is the combination of three main efficiency: the propulsive efficiency represented by SFC, the propeller efficiency η_p or the jet efficiency represented by V and, finally, the aerodynamic efficinecy $\frac{L}{D}$.

Direct Operative Cost The totality of aircraft costs directly connected to the aircraft flight. It can be seen as the amount of money necessary to carry 1 ton of payload upon 1 km.

Hierarchical Data Format A set of file formats (HDF4, HDF5) designed to store and organize large amounts of data.

Java Program toolchain for Aircraft Design Collection of libraries and classes with the aim of providing complete aircraft preliminary design analyses through the use of several semi-empirical formulas tested against experimental data.

List The `java.util.List` interface is a subtype of the `java.util.Collection` interface. It represents an ordered list of objects, meaning you can access the elements of a List in a specific order, and by an index too. You can also add the same element more than once to a List.

Map The `java.util.Map` interface represents a mapping between a key and a value. The Map interface is not a subtype of the Collection interface. Therefore it behaves a bit different from the rest of the collection types.

Parsing Parsing or syntactic analysis is the process of analysing a string of symbols, either in natural language or in computer languages, conforming to the rules of a formal grammar.

Portable Network Graphics A raster graphics file format that supports lossless data compression. PNG was created as an improved, non-patented replacement for Graphics Interchange Format (GIF), and is the most used lossless image compression format on the Internet.

Static method The term static means that the method is available at the Class level, and so does not require that an object is instantiated before it's called.

Table Is a collection that associates an ordered pair of keys, called a row key and a column key, with a single value. A table may be sparse, with only a small fraction of row key / column key pairs possessing a corresponding value.

TikZ Is a set of higher-level macros that use PGF.

True AirSpeed Is the speed of the aircraft relative to the airmass in which it is flying; TAS is the true measure of aircraft performance in cruise, thus it is the speed listed in aircraft specifications, manuals, performance comparisons, pilot reports, and every situation when cruise or endurance performance needs to be measured. It is the speed normally listed on the flight plan, also used in flight planning, before considering the effects of wind.

User developer The term refers to the developer which will use a method without being interested in how the method performs the required action. This is the case of a utility method: the developer is the one who writes the method, while the user developer is who uses that method to accomplish some action which requires the functionality provided by the utility method. It has to be noticed that the user developer and the developer can be the same person.

ACRONYMS

A.F. Autonomy Factor.

DOC Direct Operative Cost.

HDF Hierarchical Data Format.

JPAD Java Program toolchain for Aircraft Design.

MZFW Maximum Zero Fuel Weight.

PNG Portable Network Graphics.

SFC Specific Fuel Consumption.

SFCJ Jet Specific Fuel Consumption.

TAS True AirSpeed.

TikZ TikZ.

UAV Unmanned Aerial Vehicle.

LIST OF SYMBOLS

\mathcal{A} aspect ratio.

()_{cruise} quantity related to cruise condition.

η_p propeller efficiency.

()_f quantity related to flaps.

()_{LG} quantity related to the landing gear.

b span.

C_D aerodynamic drag coefficient.

C_L aerodynamic lift coefficient.

C_{D0} aerodynamic parasite drag coefficient.

D aerodynamic drag.

g gravitational acceleration.

i_W the angle between the wing root chord and the ACRF x-axis.

L aerodynamic lift.

M Mach number.

M_{ff} Fuel fraction over entire mission.

c chord.

Λ sweep.

λ taper ratio.

t thickness.

n load factor.

R range in nmi or km.

S surface.

T thrust.

V scalar velocity.

W_{OE} Operating Empty Weight.

W_{TO} Take Off Weight.

W_{fuel} Fuel Weight.

$W_{Payload}$ Payload Weight.

W weight, in N or lbf.

α_W angle of attack referred to wing root chord.

ρ air density.